



University of Tennessee, Knoxville

TRACE: Tennessee Research and Creative Exchange

Masters Theses

Graduate School

12-2007

Characterizing Groundwater-Surface Water Interactions in Great Smoky Mountains National Park using Hydrologic, Geochemical & Isotopic Data

Amanda Marie McKenna
University of Tennessee - Knoxville

Follow this and additional works at: https://trace.tennessee.edu/utk_gradthes

 Part of the [Environmental Engineering Commons](#)

Recommended Citation

McKenna, Amanda Marie, "Characterizing Groundwater-Surface Water Interactions in Great Smoky Mountains National Park using Hydrologic, Geochemical & Isotopic Data. " Master's Thesis, University of Tennessee, 2007.
https://trace.tennessee.edu/utk_gradthes/169

This Thesis is brought to you for free and open access by the Graduate School at TRACE: Tennessee Research and Creative Exchange. It has been accepted for inclusion in Masters Theses by an authorized administrator of TRACE: Tennessee Research and Creative Exchange. For more information, please contact trace@utk.edu.

To the Graduate Council:

I am submitting herewith a thesis written by Amanda Marie McKenna entitled "Characterizing Groundwater-Surface Water Interactions in Great Smoky Mountains National Park using Hydrologic, Geochemical & Isotopic Data." I have examined the final electronic copy of this thesis for form and content and recommend that it be accepted in partial fulfillment of the requirements for the degree of Master of Science, with a major in Environmental Engineering.

Randall Gentry, Major Professor

We have read this thesis and recommend its acceptance:

John Schwartz, Chris Cox

Accepted for the Council:

Carolyn R. Hodges

Vice Provost and Dean of the Graduate School

(Original signatures are on file with official student records.)

To the Graduate Council:

I am submitting herewith a thesis written by Amanda Marie McKenna entitled "Characterizing Groundwater-Surface Water Interactions in Great Smoky Mountains National Park using Hydrologic, Geochemical & Isotopic Data". I have examined the final electronic copy of this thesis for form and content and recommend that it be accepted in partial fulfillment of the requirements for the degree of Master's of Science, with a major in Environmental Engineering.

Randall Gentry, Major Professor

We have read this thesis
and recommend its acceptance:

John Schwartz

Chris Cox

Acceptance for the Council

Carolyn R. Hodges
Vice Provost & Dean of the Graduate School

(Original signatures are on file with official student records.)

CHARACTERIZING GROUNDWATER-SURFACE WATER INTERACTIONS IN GREAT
SMOKY MOUNTAINS NATIONAL PARK USING HYDROLOGIC, GEOCHEMICAL &
ISOTOPIC DATA

A Thesis
Presented for the
Master's of Science
Degree
The University of Tennessee, Knoxville

Amanda Marie McKenna
December 2007

DEDICATION

This work is dedicated to my dad who has taught me that a little sweat can go a long way.
Thank you for giving me the courage and support to go where I needed to go.

ACKNOWLEDGEMENTS

I wish to thank everyone who has aided me in attaining this Master's of Science in Environmental Engineering. Thank you, Dr. John Schwartz, for your advice as well as the use of your field equipment. Thank you, Shesh Koirala, for your lesson in proper field data collection techniques. Thank you, Candice Owen, for your time and energy in performing all of the field work with me. Thank you, Dr. Randy Gentry, for your endless patience, guidance and kindness through the research process. Finally, I would like to extend my gratitude to my family and friends who have shared my frustrations and my joys throughout these past 18 months. My experience had been valuable and meaningful because of each and every one of you. Thank you.

ABSTRACT

Groundwater-surface water interactions can substantially influence the quality of surficial water bodies and are thus important when investigating ecological health of and climate change impacts on an area. However, data collection can be hindered when the location is remote and/or legally protected. This paper presents a methodology to implement minimally-invasive field techniques at a remote and protected location that allows preliminary identification of the relationship between groundwater and surface water. Great Smoky Mountains National Park was selected as the study area as it is subjected to some of the highest rates of acid deposition in the country. Ecological damage is evident in several areas, including Ramsay Prong, a typical fourth-order stream located on the Tennessee side of the park. Ramsay Prong is evaluated on the basis of discharge, water quality, geochemistry, and stable isotopes at six points along the channel. It should be noted that increasing drought conditions occurred in the basin over the course of this study, providing an opportunity to evaluate the situation of low baseflow. Results indicate that storage capacity in the headwaters is insufficient to supply typical baseflow volume during extended dry periods, whereas sufficient alluvium exists at the bottom of the catchment to capture and recharge the basin water supply. A shallow fracture network likely provides long flowpaths for water to travel toward the basin bottom. Furthermore, baseflow is supplied by interflow as well as shallow groundwater storage; the portion of baseflow comprised by interflow increases with increasing antecedent precipitation. Diffuse groundwater recharge occurs mainly in the headwaters where steep slopes dominate the topography, while focused recharge occurs in bedrock depressions within the reaches and at the end of the channel. These observations, coupled with geochemical and isotopic data, indicate that neutralization of acidic inputs is best accomplished in the lower elevations of the basin. It is recommended that future studies investigate the ecological impacts of reduced precipitation in terms of acid neutralization capabilities along Ramsay Prong.

TABLE OF CONTENTS

1. Introduction-----	1
2. Background-----	3
2.1 Controls of Groundwater-Surface Water Interactions-----	3
2.1.1 Climatic Impacts-----	3
2.1.2 Geologic Effects -----	3
2.1.3 Topographic Influences-----	4
2.1.4 Combining Controls -----	4
2.2 Trends in Groundwater-Surface Water Interactions-----	4
2.3 Modeling Considerations -----	5
2.3.1 Study Scale -----	5
2.3.2 Hillslope Hydrology -----	5
2.3.3 Fractured Flow-----	6
2.3.4 Time Scale-----	6
3. Field Investigations -----	7
3.1 Monitoring Sites -----	7
3.2 Data Collection Methodology-----	10
3.2.1 Stream Discharge Measurement-----	10
3.2.2 Characterizing Water Quality -----	10
3.2.3 Precipitation and Drought Assessment-----	10
4. Results -----	12
4.1 Data Collection Events -----	12
4.2 Subbasin Morphology -----	12
4.3 Precipitation -----	13
4.3.1 Drought Considerations-----	13
4.3.2 Historic Patterns & Current Observations -----	13
4.4 Streamflow-----	14
4.4.1 Patterns in the Main Channel-----	14
4.4.2 Tributary Trends-----	16
4.5 Geochemistry & Water Quality -----	17
4.5.1 Water Quality -----	17
4.5.2 Dissolved Constituents-----	19
4.6 Stable Isotopes -----	24
4.6.1 Results and Influences-----	24
4.6.2 Systemic Patterns -----	25
4.6.3 Temporal Patterns -----	27
4.6.4 Spatial Patterns-----	27
5. Discussion -----	29
5.1 Drought Implications -----	29
5.2 Conceptual Model -----	29
5.3 Ecological Implications-----	30
6. Conclusions-----	31
References -----	32
Appendices -----	36
Appendix A: Raw Data -----	37
Appendix B: Sample Calculations -----	55
B.1 Ramsay Prong Discharge-----	55
B.2 Mass Loading Rate -----	55
Vita -----	57

LIST OF FIGURES

Figure 1. Location of Ramsay Prong in Great Smoky Mountains National Park, Eastern Tennessee.	8
Figure 2. Monitoring site locations along Ramsay Prong and topography of the region.	9
Figure 3. Historic monthly average precipitation and 2007 total monthly precipitation recorded at three weather stations proximate to Ramsay Prong basin.	14
Figure 4. Discharge measured in Ramsay Prong on each monitoring day.	15
Figure 5. Measured pH values in Ramsay Prong, tributaries, and adjacent springs on each monitoring day.	18
Figure 6. Measured ANC in Ramsay Prong, tributaries, and adjacent springs on each monitoring day.	18
Figure 7. Measured conductivity in Ramsay Prong, tributaries, and adjacent springs on each monitoring day.	19
Figure 8. Concentration trends with distance upstream from Site 7 for major ions in Ramsay Prong, tributaries, and adjacent springs on each monitoring day.	20
Figure 9. Concentration trends with distance upstream from Site 7 for trace metals and total silica in Ramsay Prong for each monitoring date.	21
Figure 10. Spatial relationship between deuterium and O-18 in Ramsay Prong, tributaries, and adjacent springs aggregated by location.	25
Figure 11. Temporal relationships between deuterium and O-18 in Ramsay Prong, tributaries, and adjacent springs aggregated by date.	26
Figure 12. Deuterium and O-18 patterns with distance upstream from S7 for each monitoring date.	26
Figure 13. Conceptual diagram of the flow pathways in Ramsay Prong basin below Ramsay Cascades.	29
Figure 14. Mass loading rates with distance upstream from Site 7 for major ions in Ramsay Prong, tributaries, and adjacent springs on each monitoring day.	49
Figure 15. Mass loading rates with distance upstream from Site 7 for trace metals and total silica in Ramsay Prong, tributaries, and adjacent springs on each monitoring day.	50
Figure 16. Ramsay Prong stage data measured at 15-minute intervals by the UT monitoring station sonde situated approximately 0.1mi downstream from Site 6.	54

LIST OF TABLES

Table 1. Surficial geology, elevation difference (ΔE), mean slope, and drainage area (A) per squared channel length (x^2) between monitoring sites along Ramsay Prong.	12
Table 2. Potential water-rock exchange reactions for ^2H and ^{18}O in Ramsay Prong basin.	27
Table 3. Raw velocity measurements, including distance from the bank and water depth at each point of measure, for Site 2 in Ramsay Prong on 10 April 2007.	37
Table 4. Raw velocity measurements, including distance from the bank and water depth at each point of measure, for Site 2 in Ramsay Prong on 10 July 2007.	38
Table 5. Raw velocity measurements, including distance from the bank and water depth at each point of measure, for Site 2 in Ramsay Prong on 7 August 2007.	39
Table 6. Raw velocity measurements, including distance from the bank and water depth at each point of measure, for Site 3 in Ramsay Prong on 10 April 2007.	40
Table 7. Raw velocity measurements, including distance from the bank and water depth at each point of measure, for Site 3 in Ramsay Prong on 10 July 2007.	41
Table 8. Raw velocity measurements, including distance from the bank and water depth at each point of measure, for Site 3 in Ramsay Prong on 7 August 2007.	42
Table 9. Raw velocity measurements, including distance from the bank and water depth at each point of measure, for Site 4 in Ramsay Prong on 10 April 2007.	42
Table 10. Raw velocity measurements, including distance from the bank and water depth at each point of measure, for Site 4 in Ramsay Prong on 10 July 2007.	43
Table 11. Raw velocity measurements, including distance from the bank and water depth at each point of measure, for Site 4 in Ramsay Prong on 7 August 2007.	43
Table 12. Raw velocity measurements, including distance from the bank and water depth at each point of measure, for Site 5 in Ramsay Prong on 10 April 2007.	44
Table 13. Raw velocity measurements, including distance from the bank and water depth at each point of measure, for Site 5 in Ramsay Prong on 7 August 2007.	44
Table 14. Raw velocity measurements, including distance from the bank and water depth at each point of measure, for Site 6 in Ramsay Prong on 10 April 2007.	45
Table 15. Raw velocity measurements, including distance from the bank and water depth at each point of measure, for Site 6 in Ramsay Prong on 7 August 2007.	45
Table 16. Raw velocity measurements, including distance from the bank and water depth at each point of measure, for Site 7 in Ramsay Prong on 10 April 2007.	46
Table 17. Raw velocity measurements, including distance from the bank and water depth at each point of measure, for Site 7 in Ramsay Prong on 10 July 2007.	47
Table 18. Raw velocity measurements, including distance from the bank and water depth at each point of measure, for Site 7 in Ramsay Prong on 7 August 2007.	48
Table 19. Water quality parameters recorded in precipitation throughfall near Site 6 on the bank of Ramsay Prong.	51
Table 20. Concentrations of major ions recorded in precipitation throughfall near Site 6 on the bank of Ramsay Prong.	52
Table 21. Trace metals recorded in precipitation throughfall near Site 6 on the bank of Ramsay Prong.	53

NOMENCLATURE

Units

eq	equivalents
ft	feet
km	kilometers
L	liters
m	meters
mg	milligrams
mol	moles
ppm	parts per million
s	seconds
ft/s	feet per second
L/s	liters per second
m/s	meters per second
mg/s	milligrams per second
μeq/L	microequivalents per liter
μS/cm	microSiemens per centimeter
mol·m ⁻² ·s ⁻¹	moles per meters squared per second

Abbreviations

ΔE	change in elevation
A	drainage area
ANC	acid neutralization capacity
DEM	digital elevation model
GW-SW	groundwater-surface water
GSMNP	Great Smoky Mountains National Park
K-feldspar	potassium feldspar
MWL	mean water line
NPS	National Park Service
USGS	United States Geologic Survey
VSMOW	Vienna Standard Mean Ocean Water
x	distance along reach

Chemical Species

Al ₂ Si ₂ O ₅ (OH) ₄	kaolinite clay	Mg	magnesium
Al	aluminum	Mn	manganese
Ca	calcium	N	nitrogen
Cl	chloride	Na	sodium
CO ₂	carbon dioxide	NH ₄	ammonium
Cu	copper	NO ₃	nitrate
Fe	iron	¹⁸ O, O-18	oxygen 18
² H	deuterium	P	phosphorous
H	hydrogen	S	sulfur
H ₂ O	water	Si	silicon or silica
H ₂ S	hydrogen sulfide	SiO ₂	silicon dioxide
H ₄ SiO ₄	silicic acid	SO ₄	sulfate
K	potassium	Zn	zinc
K(AlSi ₃ O ₈)	potassium feldspar		

1. Introduction

Groundwater-surface water (GW-SW) interactions are vital considerations in developing effective water resources management strategies and thus have been the focus of many studies over the past 15 years. The significance of these systems lies in their inherent ability to govern water quality and flow in adjacent streams and in the subsurface via geochemical, hydrologic and hydraulic activities. Of principle importance is the finding that GW-SW interactions can impact ecological survival, most notably for fish and benthos (Power et al. 1999; Soulsby et al. 2005; Warren et al. 2005; Boulton and Hancock 2006). This influence is the result of intense physical, chemical, and biological activities occurring within the hyporheic zone, the zone on which most research in GW-SW interactions has concentrated (Winter 1995; Sophocleous 2001). However, an understanding of GW-SW interactions throughout larger systems, such as a basin or watershed, is also important as it facilitates the evaluation of potentially adverse widespread impacts of events like irrigation and acid rain. The ability to predict these interactions is thus indispensable.

Numerous attempts have been made to mathematically model large-scale activities between groundwater and surface water, but current capabilities cannot always reproduce accurately the complexities of natural processes. Spatial and temporal variations in geology, topography, and climate have not yet been resolved numerically and, in some systems, even a conceptual understanding is difficult to ascertain. Moreover, in many locations, construction of a conceptual model may not be inhibited by system complexities but by a fundamental step in model development: data collection.

Typical methods of hydrologic data collection are not feasible in some areas of the world, namely those that are remote or legally protected. Such locations limit field observations in several capacities. Vehicles may be prohibited or physically unable to reach all areas to be evaluated, and some locales may be inaccessible by foot. Furthermore, protected lands often have designated hiking trails from which visitors are not permitted to stray; the stipulations of a permit allowing research off of the maintained path may still constrain the investigation. Additionally, weather conditions (e.g., rain events, ice, etc.) can cause inaccessibility and/or risk for injury. Overall, these limit investigations of remote and protected study areas in such aspects as: the location and number of monitoring sites, the amount and type of data collected at each site, the amount and type of equipment able to be implemented, and the longevity of the study.

Despite the challenges of performing hydrologic research in isolated and restricted areas, it is an imperative task to complete. These locations, as they are often unaltered from their natural state, may not experience environmental burdens from within their boundaries, but they can be subjected to environmental stressors from nearby sources. In particular, air emissions from coal-fired power plants, factories, and vehicle exhaust result in acid deposition that can be carried by jet streams to otherwise pristine locales. One place that exemplifies this situation is the Great Smoky Mountains.

In the Great Smoky Mountains National Park (GSMNP), characterizing hydrologic flow regimes is an important step in evaluating the effects of acid deposition and drought. GSMNP is subject to some of the highest rates of nitric (NO_3^-) and sulfuric (SO_4^{2-}) acid precipitation in the United States (Lindberg and Lovett 1992), caused by nearby power plants, factories, and automobiles. In recent years, streams and soils in the park's higher elevations have experienced especially intense acidification (Silsbee and Larson 1982; Shubzda et al. 1995) which now may be injuring ecosystem health (Flum and Nodvin 1995; Nodvin et al. 1995). Furthermore, the summer of 2007 has brought severe drought to the region (National Drought Mitigation Center 2007),

potentially attributed to global climate change. It is now critical that the hydrology of these areas be studied in order to understand (1) the role of groundwater in neutralizing acid fluxes, and (2) current ecological and geochemical equilibrium at baseflow. Both of these realizations will aid in investigating the impacts of continued acid deposition as well as permanent climate change. However, such investigations are complicated by two main features of the region: mountainous terrain and fractured rock. These not only limit field work but also make difficult prediction of hydrologic behavior. Coupling this with the fact that GSMNP is remote and protected, the challenge in the task at hand is evident.

The purpose of this study is to characterize large-scale GW-SW interactions using hydrologic, geochemical, and stable isotope data collected at several points along a main channel in GSMNP. A methodology is presented to describe baseflow patterns within subbasins of an area that is both remote and legally protected, a situation greatly limiting data availability. Specifically, Ramsay Prong of the Middle Prong Little Pigeon River Watershed is evaluated. An understanding of the relative groundwater contribution and hydrologic regime of each basin under baseflow conditions will provide insight with regard to geochemical and ecological stasis. This information will be useful to future studies of acid deposition and climate change impacts on aquatic systems both in the park and in similar areas globally.

2. Background

2.1 Controls of Groundwater-Surface Water Interactions

The primary step in developing a conceptual model is to identify the major controls on the process of interest. In the most direct sense, regional GW-SW activities are regulated by the water table configuration (i.e., the water table height compared to the elevation of the adjacent phreatic surface) and subsurface permeability (Freeze and Witherspoon 1995). However, these are governed by three rudimentary aspects of a particular region—climate, geology and topography—each impacting flow in unique yet somewhat overlapping capacities. Climate controls the amount of water on the earth's surface, while geology and topography direct the movement of water (Winter 1999). The degree of influence each exhibits is a function of location and time and can also vary by hydrogeologic scale. Thus, comprehension of the basic mechanisms by which these three affect GW-SW interactions is essential to modeling endeavors. Winter (1999) and Sophocleous (2002) provide comprehensive explanations of these activities, but a brief overview is presented below.

2.1.1 Climatic Impacts

Climate can influence water table elevation thereby altering flow direction, particularly on a local scale. For shallow aquifers, such as those adjacent to surface water, the phreatic surface elevation is reduced through transpiration and drought, while precipitation events raise the water level (Winter 1999; National Research Council 2004). As stated previously, these events also imply control of flow direction; droughts trigger groundwater upwelling, and precipitation events result in surface water seepage and aquifer recharge (Winter 1999). It should be noted that all of these activities result in only short-term trends. As groundwater is especially stable on a temporal basis, a change in weather patterns must endure decades to centuries before a significant modification in groundwater flow regime materializes (National Research Council 2004). Thus, short-term climate variations can impact aquifer recharge and discharge rates only briefly, implying that the longevity of these climate-altered GW-SW interactions is also ephemeral.

2.1.2 Geologic Effects

Geology dictates subsurface flow and transport, or, more specifically, the rate and extent of GW-SW exchange (Morris et al. 1997). Due to natural variations in geologic properties, such as porosity, grain-size, mineralogy, and soil saturation, an aquifer's hydraulic conductivity as well as storage capabilities can exhibit a broad range of values. This is especially true in areas comprised of fractured rock. One of the main challenges in modeling hydrologic activities in a location comprised of fractures is scale. A regional study may capture a large fracture network that does not uniformly extend throughout the watershed, and down-scaling observations could lead to overestimation of subsurface flow (if the local site of interest is not connected to the main fracture network). Similarly, observations from a local study cannot be accurately extrapolated to a regional perspective (Nastev et al. 2004; National Research Council 2004). It is therefore the scale of the problem that determines the extent of the geology for which to account (Eaton 2006).

Effects of geologic heterogeneity also apply to processes at hydrologic boundaries, manifesting as recharge and discharge that are either diffuse or focused. In general, diffuse flux is supplied by porous media (e.g., soil), while gaping features, such as rock fractures and karst, promote focused flow. Focused recharge, in particular, is also generated by surficial depressions and unsaturated zones (National Research Council 2004). Furthermore, as fracture networks are not always connected to the land surface, these discrete flowpaths can control the exact location of recharge and discharge; streamflow can disappear into a fracture and not emerge

for miles. Hence, the geology of any location greatly influences the rate of flow both into and out of the system.

2.1.3 Topographic Influences

Topography manipulates flow due to changes in hydrological response with landscape geometry (Hilberts et al. 2004). Mountainous terrain is unique in that, due to a non-horizontal geologic boundary, it has the ability to generate flow. Studies show that surficial runoff mainly depends on the amount of precipitation and antecedent soil moisture (i.e., soil moisture prior to a precipitation event) (Buttle et al. 2004; Tromp-van Meerveld and McDonnell 2006a; Tromp-van Meerveld and McDonnell 2006b). Yet, it is not simply the external land slope that controls flow generation down the hillslope; the internal geologic features and overlying soil thickness also contribute. This is well-illustrated through several trench studies of stormflow in mountainous terrain. Most notably, Tromp-van Meerveld and McDonnell (2006a, 2006b), who examined hillslope response of 147 storms, concluded that during a precipitation event, bedrock depressions fill and may subsequently spill over the downward slope, creating a relatively large water flux within the subsurface. This “fill and spill hypothesis” implies that although subsurface flow depends upon total precipitation and soil moisture, these fluxes are also a function of bedrock topography (Buttle et al. 2004; Tromp-van Meerveld and McDonnell 2006a). Connection of the hillslope to nearby streams can thus be limited by the underlying bedrock, particularly when the storage threshold is infrequently attained.

2.1.4 Combining Controls

It is within these internal and external hydrogeologic factors that challenges in developing a conceptual understanding of the system arise. Precipitation may be concentrated on the mountain front and/or in high elevations due to orographic effects (Wilson and Guan 2004). The degree of hillslope can change locally and regionally. Soil thickness is not always uniform, inducing variations in soil moisture with space and time. Bedrock depressions may store water, releasing flow only when certain moisture conditions are attained; a single hillslope may exhibit any combination of number and sizes of depressions (Tromp-van Meerveld and McDonnell 2006b). Furthermore, bedrock may contain areas of fractured rock in which case the speed and direction of water are dictated by the connectivity and magnitude of the fractures and their exchanges with pockets of porous media (Berkowitz 2002). Coupling all of these factors and their arrays of possible values, the difficulty in developing a conceptual hydrologic model of a fractured hillslope is evident, particularly when geologic information is unavailable or limited.

2.2 Trends in Groundwater-Surface Water Interactions

As Sophocleous (2002) and Silvapalan (2003) point out, a need to catalog hydrologic patterns based on general combinations of geology, topography, and climate exists. Such conceptual models will not only assist in characterizing simple, homogenous systems but will also facilitate a fundamental understanding of the complex ones.

The few studies that have attempted to standardize trends in GW-SW interactions typically categorize their results by geology or topography. The aim has been to compare within similar geologic settings (of differing climate and/or topography) and subsequently search for patterns between settings. For instance, Vidon and Hill (2004) examined the links between topography, aquifer thickness and geology in glacial outwash. Results indicated that an increase in hillslope produces elevated subsurface fluxes through the riparian zone as well as the prohibition of flow direction reversals (surface water to groundwater) during dry periods. Winter (1999) summarizes the effects of climate and geology on GW-SW interactions in an assortment of terrains, concluding that although the same fundamental mechanisms (e.g., seepage, transpiration, recharge, etc.) may occur in every geology type, the extent and relative influence of each process may differ. This observation is indicative of the need for an

extensive library of research, observing all combinations of topography, climate and geology, to further the comprehension of GW-SW interactions.

2.3 Modeling Considerations

As previously stated, model development is steered by the identified process controls. A GW-SW model, in particular, accounts for its controls of climate, geology and topography through four elements: scale, landscape (i.e., terrain), heterogeneity and time. Although ultimately based on study site characteristics, selection of the specificities of these elements is accomplished by considering the investigation goals. In this case, a Smoky Mountain watershed subbasin exhibiting fractured geology is examined under baseflow conditions. The following addresses the specific needs in developing a conceptual understanding of the region.

2.3.1 Study Scale

Objectives of an investigation coupled with physical boundaries define the study scale. This parameter is critical in recognizing the appropriate level of detail to consider; a microscopic nuance would not be considered when conducting a regional study.

The scale of a natural flow system can be categorized in one of three hierarchical classes: local, intermediate or regional (Tóth 1963). The main difference in local and intermediate flow systems is that while both discharge to a nearby water body, intermediate flow systems include at least one topographic high and low situated between the main recharge and discharge locations. It should be noted that these topographic maximum and minimum are not the major topographic high and basin bottom, respectively; such extremes are boundaries of the regional flow system (Tóth 1963).

The Middle Prong Little Pigeon River Watershed is a regional flow system. However, as only the area directly surrounding Ramsay Prong is examined, the study scale is classified as intermediate. It is further divided into smaller segments, termed subbasins, to analyze macroscopic local interactions.

2.3.2 Hillslope Hydrology

The principal concern in modeling mountainous terrain is accurately describing the distribution of aquifer recharge and discharge. In a system exhibiting significant topographic relief, recharge (i.e., precipitation) concentrates in higher elevations (Winter 1999; Wilson and Guan 2004), while discharge materializes in lower elevations as streamflow or springs (Winter 1999). In effect, water is funneled downhill and collects in a lower area of the system (Winter et al. 1998). Consequentially, recharge can also come from streamflow, particularly when the hydraulic head of the channel exceeds that of the adjacent water table (Winter 1999).

Due to the funneling of water to lower elevations (Winter 1999; Winter et al. 1998), the type of aquifer recharge can change throughout the basin. Diffuse (i.e., dispersed) infiltration may dominate in higher altitudes where precipitation is distributed and the sloping terrain mitigates pooling. On the other hand, focused (i.e., concentrated) aquifer recharge occurs at lower elevations because—due to the retreating hillslope—the water is captured and ponds. These patterns can be enhanced by poor storage qualities of the upstream subbasins compared to typical alluvium found at the base of a hillslope.

The Ramsay Prong basin is located within an area of substantial topographic relief, indicating that precipitation may vary spatially. However, as this investigation evaluates baseflow conditions only, a quantitative assessment of precipitation is irrelevant. Instead, data from proximate weather monitoring stations are used for qualitative analysis. Patterns in streamflow are implemented to identify areas of diffuse and focused groundwater recharge.

2.3.3 Fractured Flow

Flow through fractured rock differs from flow through porous media in three key, interconnected facets: storativity, geochemical signature, and flux type (Mayer and Sharp 1998). The underlying premise that joins these elements is the fact that fractured rock provides uninhibited flowpaths for water to travel. As such, hydraulic residence time (storage) is relatively brief in shallow aquifers (i.e., depths at which GW-SW interactions mainly occur), prohibiting extensive reactions between the rock-water interfaces. This indicates that—assuming precipitation contains a negligible amount of dissolved mineral species—the concentration of ions in water from fractured networks is typically less in comparison to water from deep aquifer storage or porous media; geochemical equilibria are unattained with such brief residence time.

With regard to flux type, uninhibited flowpaths facilitate focused recharge and discharge, as opposed to diffuse flux exhibited by porous media. Such discrete fluxes may be indicated by significant changes in streamflow (magnitude and geochemistry) over a short reach length. However, beyond a local scale, flow is dictated by the connectivity and density of fractures (Berkowitz 2002), indicating two pertinent concepts. First, storage in a fractured system can be highly variable on a spatial basis. Second, as fractured rock can allow significant vertical flow (increasing with fracture size) (Oxtobee and Novakowski 2003), water can be routed to unpredictable locales, even across hydrologic divides, or can be lost to deep aquifers. Thus, an observed loss in channel discharge may not reappear in the same stream or even same basin, and, similarly, a gain of streamflow may not have sourced from the stream under investigation (Tóth 1963; Winter et al. 1998). Considering these possibilities, any characterization of GW-SW activities must begin by locating fractures and realizing their connectivity. However, an underlying problem currently exists here: fractures cannot be directly measured.

Aerial photographs, core samples, fractured outcrop observations, tracer tests, and geophysical techniques are helpful tools for delineating fracture networks but are incomplete. Models, therefore, rely on assumptions and extrapolations that may not accurately describe the fractured region as local observations may not represent regional trends. Even in well-understood systems, the irregularities of fractures and fracture networks inhibit up-scaling of observations (Nastev et al. 2004). It is thus the limited amount of collectable data that impedes comprehension of fractured flow. However, a conceptual hydrologic model in such a complicated system is often a primary necessity, particularly places that are experiencing some type of environmental burden. For instance, areas of rapid flow may not be able to mitigate the effects of acid rain. GSMNP may typify this condition.

As Mayer and Sharp (1998) point out, a priori knowledge of the locations and sizes of fractures can significantly enhance these modeling endeavors, particularly in highly erratic fracture networks. For this work, geologic maps of soil and bedrock in addition to field observations are implemented to infer the existence and potential regional patterns of fractures in the domain. Coupled with geochemical analyses, isotopic concentrations and discharge observations, this knowledge will aid in locating areas of groundwater contribution to the channel.

2.3.4 Time Scale

Two temporal categories of groundwater-surface water interactions exist: short-term and long-term (Mitchell-Bruker 1996). While predictions of short-term interactions are important for predicting stormflow, modeling long-term processes illustrates overall groundwater flow as well as average baseflow in stream networks. This study characterizes only long-term, steady-state interactions as it is the project goal to examine baseflow patterns. Such investigation will shed light upon hydrologic and geochemical fluxes during a state of equilibrium flow.

3. Field Investigations

The site chosen for investigation is the Ramsay Prong of the Middle Prong of the Little Pigeon River, located in the Greenbrier Valley (Middle Prong Little Pigeon River Watershed) of eastern Tennessee (Sevier County). Figure 1 illustrates the location of this catchment with respect to GSMNP.

This region is part of Great Smoky Mountains National Park and is a wilderness-designated area accessible only by a steep maintained foot trail. The particular reach under investigation lies approximately 6 miles west of Gatlinburg. It begins at the Ramsay Cascades—elevation 1300m (4280ft)—and extends to the intersection of Ramsay Prong and Middle Prong—elevation 950m (2620ft). Forests chiefly comprised of hickory, oak, and yellow pine species—untouched for the past century—fill the basin. Climate in this region is temperate. Annual precipitation averages 138-216cm (55-85in) per year, increasing with altitude. Temperature typically ranges from -10°C (13°F) in the winter to 30°C (85°F) in the summer (National Park Service 2006).

The Ramsay Prong basin is surficially comprised of Ditney-Unicoi-Spivey soils, thin, sandy loams typically less than 1m (3.3ft) thick characterized by moderately rapid permeability and medium surficial runoff, while the underlying bedrock consists of Thunderhead Sandstone (Soil Data Mart 2007). As described by the USGS (Southworth 2005), Thunderhead Sandstone is thickly-bedded, fine-grained conglomerate with graded beds of coarse-grained metasandstone that are interbedded with dark-colored metasilstone. The dominant minerals within the formation are quartz and potassium feldspar (i.e., K-feldspar). Boulders of dark-colored slate and dolomite occur locally.

Ramsay Prong is a typical fourth-order, high-gradient mountainous stream. The section of interest begins at the base of Ramsay Cascades, an 18m (60ft) high wall of Thunderhead Sandstone dipping away from the base at approximately 30 degrees (Moore 1995). Colluvial and alluvial boulders spot the stream bed and outline the banks, slightly reducing in number and size toward the confluence of Ramsay Prong and Middle Prong. At present, only a portion of the surficial deposits in the Ramsay Prong basin have been mapped (Soil Data Mart 2007). The incomplete data does show, however, that the site just before the confluence with Middle Prong (S7) sits in a fan of Pleistocene alluvium. Also illustrated by the data is that two of the middle sites (S3, S4) are dominated by Holocene and Pleistocene colluvium. From observation during field work and extrapolation from USGS data, the other two middle sites (S5, S6) exhibit the same, while the site at Ramsay Cascades (S2) is characterized by large sandstone outcrops and colluvium.

It should be noted that at the time of this study Eastern Tennessee, including Middle Prong Little Pigeon River Watershed, transitioned from an abnormally dry period to a state of extreme drought (National Drought Mitigation Center 2007). This implies that the quantitative values of this study may not illustrate the stable trends of the past but a transition into a drier climate. However, flow patterns should be similar as the drought has endured only a few months; tens to hundreds of years are required for significant changes in hydrologic flow regimes to occur (National Research Council 2004).

3.1 Monitoring Sites

For this study, Ramsay Prong is divided into subbasins based on the location of major inputs to the stream. These inputs were determined as: Ramsay Cascades, two tributaries along Ramsay Prong, and the confluence of Ramsay Prong and Middle Prong. Monitoring sites were located

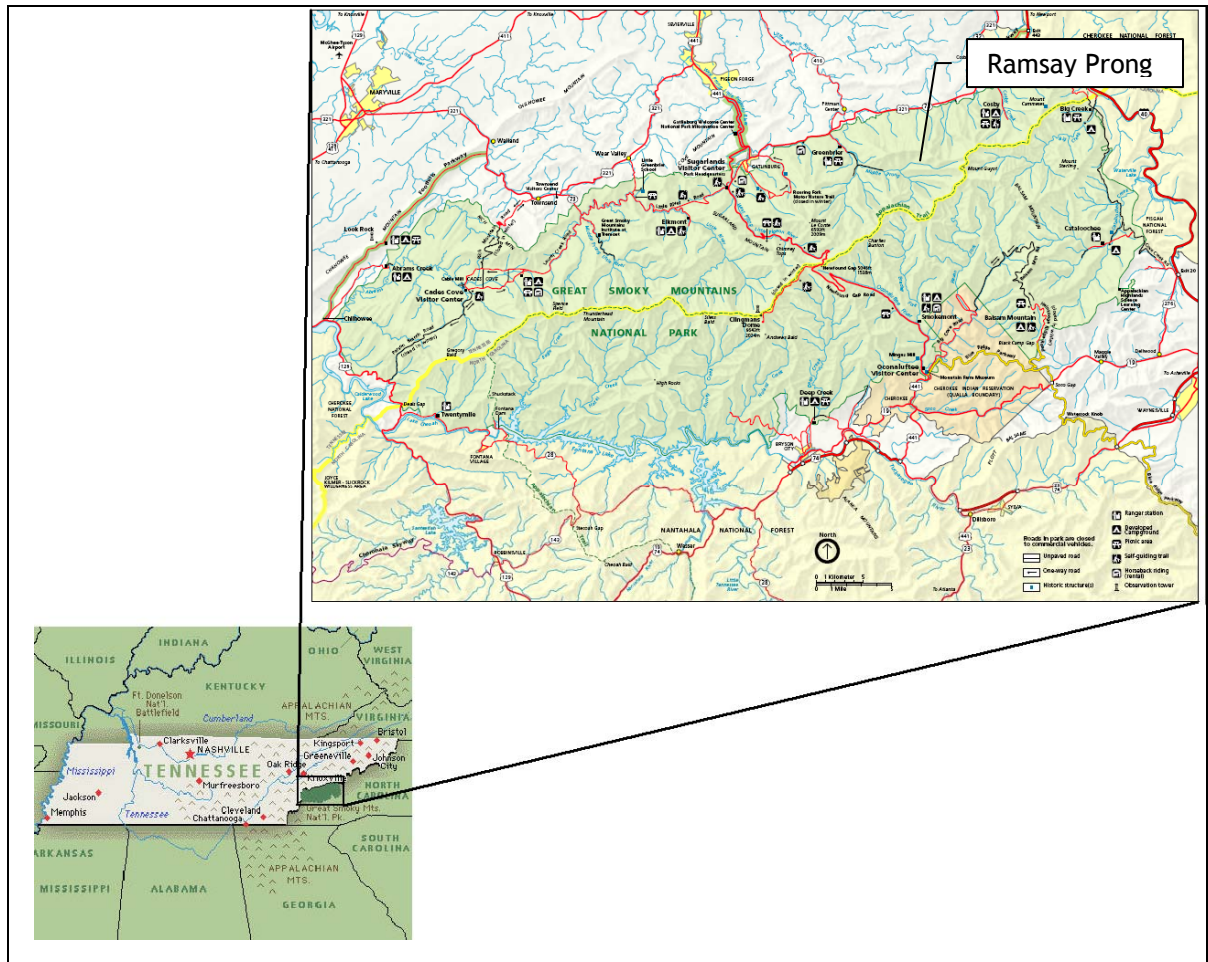


Figure 1. Location of Ramsay Prong in Great Smoky Mountains National Park, Eastern Tennessee. Tennessee regional map (left) accessed from <http://www.greenwichmeantime.com/time-zone/usa/tennessee/map.htm>. Great Smoky Mountains National Park (right) illustration courtesy of the National Park Service (2006).

directly downstream of the cascades (S2), upstream and downstream of the tributaries (S3, S4, S5, S6), and upstream of the confluence (S7), producing six monitoring points and thus six subbasins along the reach. Tributary 2 (T2) is located between S3 and S4, while Tributary 3 (T3) sits between S5 and S6. A monitoring station just below Tributary 1 (T1) was also desired, but the area proved unreachable for safety reasons. Furthermore, a site (S1) above Ramsay Cascades was also considered but found unreachable due to the trail's culmination and ensuing hazardous terrain (e.g., steep slope and rock walls). Figure 2 describes the monitoring locations.

Water samples were also collected from Tributaries 1, 2 and 3, as well as a spring located approximately midway between S6 and S7. It should be noted that only T1 was sampled on all three monitoring events. The spring had dried up after April, and it was not thought to sample T2 and T3 until August.

As depicted by the U.S. Geological Survey's digital elevation model (DEM) used to create Figure 2, two additional tributaries appear to exist just downstream of S4. However, these channels were not found in the field. It is therefore assumed that the DEM lines represent minor drainage paths (i.e., wet weather conveyance) that materialize as springs or seeps along the hillslope. However, these potential discharges could not be located despite lengthy reconnaissance.

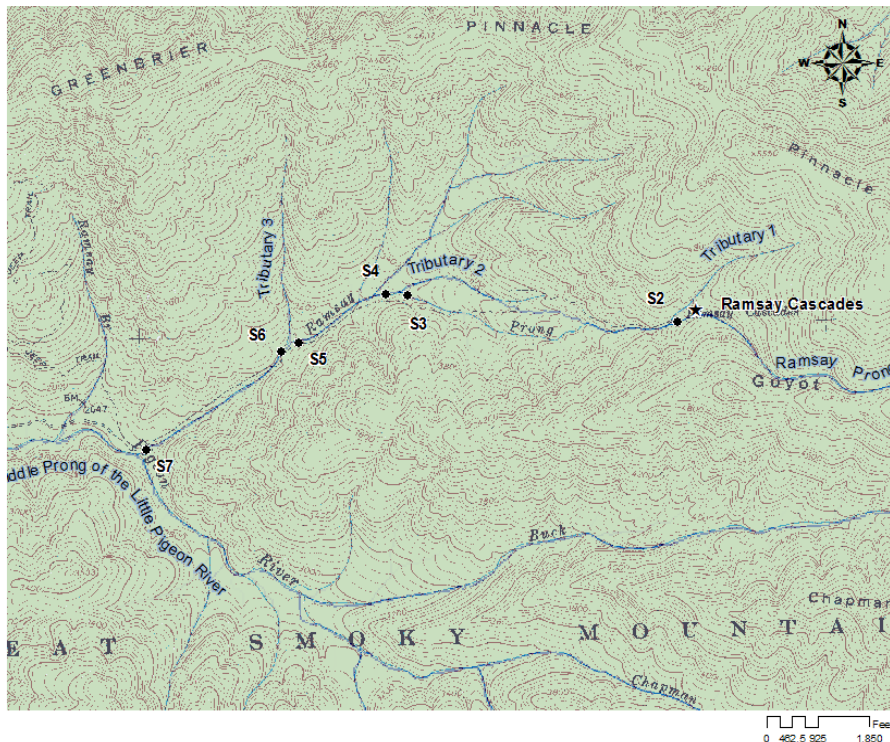


Figure 2. Monitoring site locations along Ramsay Prong and topography of the region.

3.2 Data Collection Methodology

Information describing Ramsay Prong basin was garnered through online databases as well as in the field. Stream discharge, water quality parameters, and concentrations of major ions and isotopes were interpreted from site measurements, while precipitation was approximated from nearby weather stations. Drought conditions were assessed from the U.S. Drought Monitor (2007). At least 48 hours were allowed after a storm event before collecting data in order to ensure that baseflow conditions had returned.

3.2.1 Stream Discharge Measurement

Streamflow data was collected along Ramsay Prong on several days dispersed throughout the 2007 field season. Velocity and depth were measured to calculate discharge as per the USGS Six-Tenths-Depth method (Buchanan and Somers 1976). These parameters were recorded at intervals of 0.3m (1ft) or 0.6m (2ft) across Ramsay Prong, depending on the local width of the stream; a wide section was observed at the greater interval. Depth was measured with a round wading rod and velocity by a portable flow meter (FLO-MATE Model 2000, Marsh-McBirney, Inc.) attached to the submerged end of the wading rod. Discharge was subsequently estimated as the area under the curve on the plot of distance from bank (x) against velocity (y).

3.2.2 Characterizing Water Quality

Water quality parameters were quantified with a YSI Hydrolab (Model 556 MSP), as reported by Owen (2007). Values for water temperature, pH, dissolved oxygen, and conductivity were recorded once at each site during each visit. This was accomplished by placing the probe at a position in each cross-section that allows it to be fully submerged yet not in contact with the stream bed, stream banks, or any obstruction (i.e., boulders) within the stream. In essence, the probe was in forward-flowing, relatively deep water. It should be noted that the pH meter did not seem to function properly, so the values reported in this document are those of the collected water samples (described below) as measured by the laboratory at the University of Tennessee.

A water sample was collected at each of the six monitoring points for laboratory analysis of acid neutralization capacity (ANC), conductivity, pH, major ions (Ca, Mg, Na, K, NH₄, SO₄, NO₃, Cl), total silica (Si) and trace metals (Al, Cu, Zn, Fe, and Mn), as well as stable oxygen (O-18) and hydrogen (deuterium) isotopes, ¹⁸O and ²H, respectively. Values for each of these parameters, except the isotope concentrations, were originally reported in Owen (2007). ANC, conductivity, and pH were measured with a Mantech PC-Titration Plus instrument. Anions were evaluated with a Dionex Ion Chromatograph, while cations and metals are analyzed with a Thermo-Elemental iris Intrepid II ICP. A Finnigan Delta Plus, dual inlet, coupled with an Equilibrator Mass Spectrometer measured the stable isotope concentrations, reporting as per mil (‰) deviations (δ) from the international Vienna Standard Mean Oceanic Water (VSMOW). Precision is at least 0.05‰ for O-18 and at least 1.0‰ for deuterium.

3.2.3 Precipitation and Drought Assessment

Precipitation data is collected by the National Park Service (NPS) weather stations at several locations throughout the park. However, only two of these stations are located nearby Ramsay Prong, and regionalization techniques would be unfounded, particularly because both stations sit on the western side, prohibiting accurate extrapolation to the basin. Precipitation was thus evaluated on a qualitative basis only.

The U.S. Drought Monitor (2007) has been implemented to assess the hydrological state that the region (i.e., Sevier County, TN) experiences during the investigations. This tool rates an area on a hierarchical scale of drought severity. From least to most severe, the categories are: *Abnormally Dry* (D0), *Moderate* (D1), *Severe* (D2), *Extreme* (D3), and *Exceptional* (D4). These

correspond to Palmer Indices of -1.0 to -1.0, -2.0 to -2.9, -3.0 to -3.9, -4.0 to -4.9, and -5.0 or less, respectively (U.S. Drought Monitor, 2007). Note that the U.S. Drought Monitor is not simply a qualitative representation of the Palmer Index but is an assessment of several indices, including the CPC Soil Moisture Model, Standardized Precipitation Index, USGS Weekly Streamflow Percentiles, and Short-Term and Long-Term Drought Indicator Blends (National Drought Mitigation Center 2007), suggesting its reports provide a comprehensive evaluation of drought conditions.

4. Results

4.1 Data Collection Events

Field data was collected on three days dispersed throughout the 2007 field season: April 10, July 10, and August 7. Data was also to be gathered in mid February, but icy conditions in the stream presented too great of a risk for injury, and no information was able to be safely obtained. It should be noted that a storm event in the afternoon of July 10 prohibited monitoring sites 5 and 6 from being sampled; the rain began before the sites were accessed. Information from the other sites on this date is presented as it is still valuable.

4.2 Subbasin Morphology

In order to explain observed flow patterns in the Ramsay Prong basin, each stream reach must be characterized in terms of geology, topography, and relative size. Table 1 presents physical descriptions of each subbasin based on field observations, soil maps from the Natural Resources Conservation Service Soil Data Mart (2007), and the USGS DEM pictured in Figure 2.

It is apparent that the higher elevations are characterized by relatively steep slopes and a predominance of large boulders and rock outcrops. Moving down in the basin, slopes flatten out, and a layer of weathered residuum develops. These observations imply that storage in the lower altitudes may be better facilitated than near the cascades.

Table 1. Surficial geology, elevation difference (ΔE), mean slope, and drainage area (A) per squared channel length (x^2) between monitoring sites along Ramsay Prong.

Reach*	Surficial Geology	ΔE (m)	Mean Slope (%)	A/x^2
S2+	<ul style="list-style-type: none">many rock outcrops & large bouldersvery thin layer of soil	707	15.2	0.16
S4-S2	<ul style="list-style-type: none">upstream contains many rock outcrops & large boulders with a thin layer of soiltransitions to colluvial debris and a somewhat thicker soil layer downstream	360	22.0	0.84
S6-S4	<ul style="list-style-type: none">dominated by colluvial debristhin soil layer	27	3.90	7.85
S7-S6	<ul style="list-style-type: none">upstream is comprised of colluvial debris with a thin soil layertransitions to an alluvial fan downstream with a slightly thicker soil layer	119	12.3	0.93

*Reach S2+ represents the catchment area between the start of Ramsay Prong and S2.

4.3 Precipitation

As this study analyzes baseflow, the magnitude of precipitation is only important with regard to the drought. Thus, data is reported in a predominantly qualitative fashion. Chemistry of rainwater is also important as it is required to understand the chemical evolution of water in Ramsay Prong basin.

4.3.1 Drought Considerations

Drought conditions began to immerse at the beginning of February 2007 when the U.S. Drought Monitor first ranked Sevier County as *abnormally dry*. A week later, the status increased to *moderate*, implying low well levels and developing water shortages, and remained there until the first week of May (U.S. Drought Monitor, 2007). However, field investigations on April 10 most likely occurred under normal baseflow conditions as the drought had not yet significantly impacted the region. However, by the first week of May this rating had jumped two categories to *extreme*—meaning widespread water shortages or restrictions (U.S. Drought Monitor, 2007), and have not yet changed. This indicates that investigations carried out on July 10 may illustrate reduced baseflow. As the *extreme* categorization continued through to the final field day, data from August 7 may illustrate even lower baseflow conditions. Again, despite the reduced baseflow situation, dominant GW-SW exchange patterns have most likely not been altered.

4.3.2 Historic Patterns & Current Observations

Precipitation data is estimated based on the most proximate weather stations to Ramsay Prong basin. Records from a University of Tennessee field monitoring site near S6 are utilized to infer throughfall chemistry along the channel; these values are located in Appendix A. Precipitation volume is approximated from data collected at GSMNP Headquarters at Sugarland Center—elevation 541m (1775ft)—and Newfound Gap—elevation 1566m (5138ft). However, a complete data set for rainfall volume over the period of investigation was inaccessible, so records from the University of Tennessee's Gatlinburg weather station are used for qualitative assessments. Sugarland Center, Newfound Gap, and Gatlinburg are shown in Figure 1.

Except for the Gatlinburg setting, the stations' altitudes capture the elevations of this investigation's monitoring sites (950-1300m), indicating that the recorded data represents the range of precipitation to which the basin is most likely subjected. Gatlinburg precipitation data is used only as a reference to the relative amount of precipitation Ramsay Prong basin may have received. The NPS record for total monthly precipitation averaged over more than a decade is plotted against the 2007 monthly totals in Figure 3.

Since Gatlinburg precipitation generally follows the historic magnitudes and trends at Sugarland Center, the former station can be used to predict the amount of precipitation incurred by the basin. For the study, this parameter is assumed to follow the patterns seen at Gatlinburg with volume of precipitation increasing roughly linearly with altitude. On average, the basin received probably only half of its usual amount of precipitation over the course of this study. Drought conditions are thus evident.

Under the assumption that precipitation increases linearly with elevation, it follows that the amount of dissolved species, such as nitrate and sulfate, found in stream water would also rise with altitude. A year-long study conducted in the Noland Divide Watershed of GSMNP indicated that although this assumption was true for sulfate, total inorganic nitrogen (NO_3^- and NH_4^+) was significantly greater in the lower site (located at ~1740m) (Shubzda et al. 1995). This observation was attributed to a superior rate of canopy uptake in the upper site (located at ~1920m). In the current study, because throughfall is measured at the second lowest site (S6) and the elevation difference to S2 is much greater than the difference in the Noland Divide

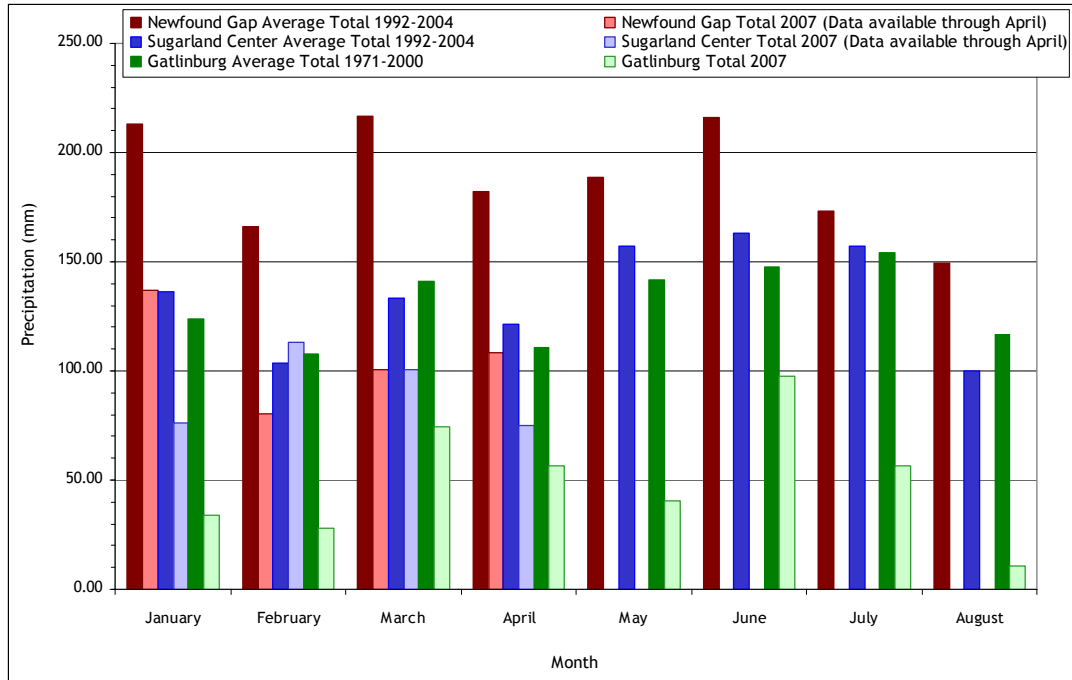


Figure 3. Historic monthly average precipitation and 2007 total monthly precipitation recorded at three weather stations proximate to Ramsay Prong basin.

study (~1300m versus ~200m, respectively), total nitrate measured here is considered the maximum possible within Ramsay Prong basin. Similarly, recorded concentrations of sulfate and all other dissolved species in throughfall are considered minimums such that Ramsay Cascades was subjected to the greatest rates of deposition. Similarly, it is assumed that pH decreased with increasing altitude. Throughfall chemistry records are found in Tables 19-21 in Appendix A.

4.4 Streamflow

As expected, stream discharge typically increased: (1) at a point directly following a tributary and (2) overall from S2 to S7. Streamflow between observation days at each site showed obvious variation moving downstream with a particularly large magnitude at S7. Such apparent temporal fluctuations occurred in the tributary flow magnitudes, as well. These variations are typical when headwaters are underlain by a low permeability geologic unit (Winter 2007). Figure 4 presents the discharge trends of Ramsay Prong during the course of the study.

4.4.1 Patterns in the Main Channel

Although the magnitude of streamflow increases overall from the top of the basin to the bottom, each subbasin does not necessarily exhibit an increase in discharge. Flow in the headwaters (S2-S3), in particular, is relatively stable during the months when the drought was most prominent (i.e., July and August). However, in April, prior to extended drought conditions, baseflow was relatively low. This occurrence was most probably the result of groundwater storage depletion due to insufficient recharge; total monthly precipitation was

substantially low—even exhibiting a value of zero—during early spring. Supporting this claim is the observation that baseflow at S2 climbed in July (after storage replenishment by June storm events) but had dwindled by August (when the prior month’s rainfall was much less than average) to a discharge between those of July and April. Nevertheless, the headwaters are able to supply at least some baseflow even during severe drought, potentially sourcing from an area above S2; uninterrupted flow over the cascades was observed during all three monitoring days as well as during the February investigation.

The relatively large decline in discharge between S2-S3 from April to August implies that another mechanism influences flow in this subbasin. As this pattern is strictly temporal, the reduction in additional flow may be attributed to drought. Specifically, T1 as well as local springs experienced diminished flow with extended drought, decreasing or even eliminating their baseflow contribution to the main channel. This lack of additional inputs along the reach over time ultimately caused a shorter jump in flow from S2 to S3.

Contrasting flow observations in the reach between S4 and S5 reveal a key attribute of the subbasin. The change between a losing to gaining reach signifies that this is an area where groundwater storage cannot always maintain baseflow (Brunke and Gonser 1997; Fetter 2001). Since the groundwater reservoir in the basin was low in April, as explained above, water in this reach infiltrated as recharge. By August, the stream had replenished the aquifer, and baseflow was again being supplied by storage. The observation that the groundwater reservoir between

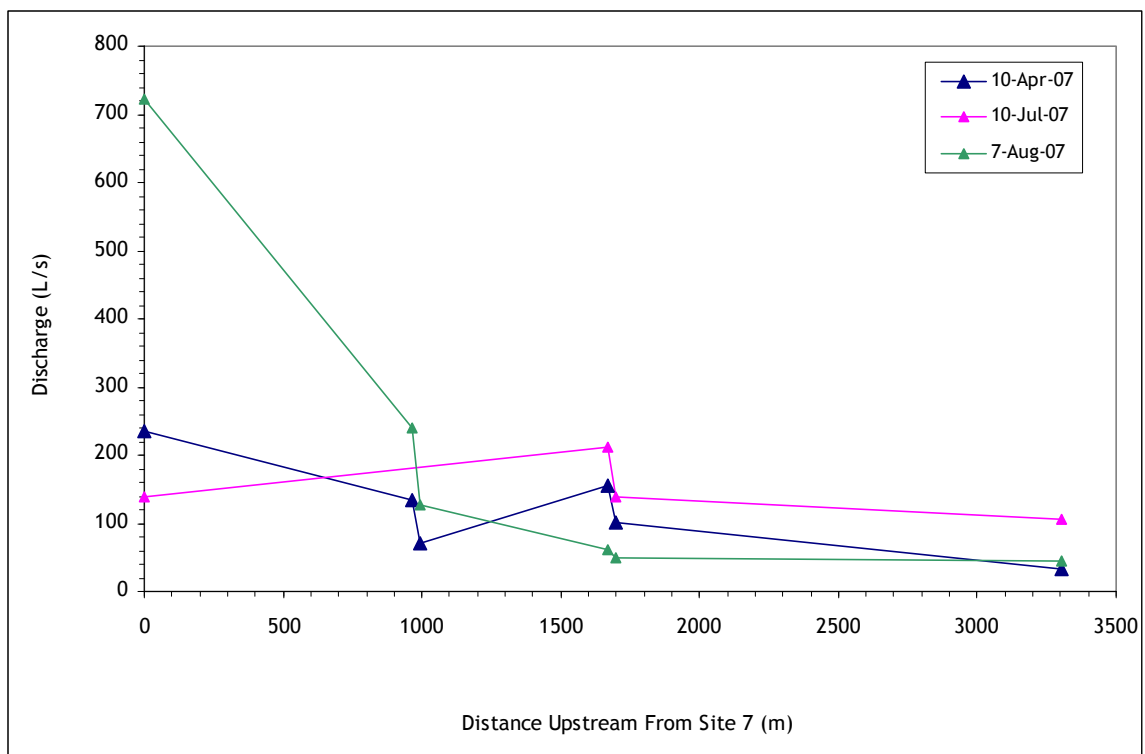


Figure 4. Discharge measured in Ramsay Prong on each monitoring day.

S4 and S5 filled even during a time of drought also suggests that flow is being captured here without immediate release downslope. This pattern is reflected by the change in discharge over the final reach (S6-S7), as well. During losing conditions, the final streamflow (at S7) recovered by only a small amount, while gaining conditions displayed a markedly elevated final discharge. Such a climb in flow is attributed to the fact that baseflow was being supplied (not recharging) along reach S4-S5. Although July data is incomplete, its trend from S4 to S7 suggests a refilling aquifer, as well. Flow does not completely recover in this case, though, illustrating that the volume of stored water had been even more depleted. These trends are similar to observations by Tromp-van Meerveld and McDonnell (2006a; 2006b) and imply that their Fill and Spill Theory may be applicable to this Smoky Mountain basin. In effect, a large storage area (i.e., bedrock depressions, a fractured rock unit, etc.) between S4 and S6 must fill (and subsequently spill over) before the remaining portion of the catchment has a continuous hydrologic link to the upper parts of the basin. Furthermore, the relative stability in August discharge implies a greater contribution of storage from the saturated zone than during the other monitoring dates (Winter 2007).

Despite being subjected to the smallest volume of antecedent precipitation, the August monitoring event was characterized by the greatest volume of streamflow at the bottom of the basin. Such an observation appears counterintuitive but was confirmed with visual observations during the field investigations: the average recorded water depth was at least three times that seen in April or July. This implies that a delaying mechanism exists between the headwaters and catchment bottom, again pointing to the idea that Tromp-van Meerveld and McDonnell's (2006a; 2006b) Fill and Spill Theory applies to Ramsay Prong basin. In April and July, the storage was not at capacity, so the stream reach lost water to the area, and the basin bottom (i.e., S7) received little to no flux of water from the capture region. However, between July and August, high-elevation interflow coupled with additional precipitation had worked its way to the lower altitudes and filled the storage area. Thus, in August, the hydraulic head in the storage met the unsaturated zone such that the stream gained water.

The differing rates of change in discharge between reaches S2-S3 and S4-S5 are attributed to basin morphology. Specifically, these differences are due to slope and soil cover. In the higher reach (S2-S3), the average slope is over five times greater than that of the lower reach (S4-S5) and is characterized by a thin layer of sandy loam underlain by solid rock (Soil Data Mart 2007). As Fetter (2001) points out, such a circumstance facilitates rapid fluxes down the hillslope. In contrast, water slows and even ponds in the lower reach due to a combination of flatter slopes and the relative abundance of weathered rock residuum. This creates an opportunity for considerable exchange between the surficial water and subsurface storage components, particularly if the storage unit is shallow.

The discharge pattern can be minimally ascertained by stage data garnered at the UT field monitoring station situated approximately 0.1mi downstream of S6. Records from this investigation, as shown in Table 14 and Table 15 of Appendix A, indicated that the flow at S6 was higher in August than in April. Stage measurements by the UT field station confirm this, as seen in Figure 16 of Appendix A. Since no data was able to be obtained in July at S6, no comparison of the manual records with the monitoring station value can be performed.

4.4.2 Tributary Trends

It is assumed that the flow contribution of a tributary to Ramsay Prong is the difference in discharge between monitoring sites directly surrounding the tributary. In other words, the flow difference between S3-S4 is T2's input, and the flow difference between S5-S6 is T3's input. As such, temporal flow trends in tributaries 2 and 3 follow those in the stream reaches.

In April and July, when high elevation springs and streams had not yet dried, T2 flowed soundly. However, by August, the volume of T2 was reduced because of drought conditions, just as the springs along S2-S3 had dried.

Tributary 3 displayed constant flow during early spring as well as in August. Similar to streamflow trends, August streamflow did exhibit a higher volume, implying again that the amount of stored water had risen.

4.5 Geochemistry & Water Quality

4.5.1 Water Quality

Water quality parameters for the main channel, tributaries, and spring exhibited generally steady trends while moving downstream; they appear in Figures 5, 6, and 7. The data implemented to create these plots is located in Owen (2007)

The small spatial decrease in conductivity, despite an overall rise in mass loading rate, simply reflects a slight drop in total ionic concentration, while on a temporal basis, the rise of conductivity with greater antecedent precipitation indicates that larger masses of dissolved species are flushed into baseflow with increasing volume of antecedent precipitation. Coupling these observations, it is not surprising that the highest elevations exhibit the greatest conductivity as these areas receive a larger amount of precipitation and thus a larger mass of dissolved species. This is contrary to a study to assess the mean catchment properties in GSMNP that observed no significant trend in conductivity with altitude (Silsbee and Larson 1982). However, conductivity in the present study changed so minimally, it may be concluded that no statistically significant pattern was observed.

The ANC rose from the top of the basin to the bottom because of geologic differences between these areas. Brief residence times in the higher altitudes (caused by steep slopes and shallow soil depths) do not facilitate neutralization capabilities, whereas delayed flow (caused by flatter terrain and deeper pockets of colluvial/alluvial debris) in the lower parts of the basin induce longer residence times, whereby acidic inputs are more apt to be neutralized via geochemical exchanges. Additionally, temporal trends signify that the composition of baseflow during drought (i.e., August) is more effective at neutralizing acidic inputs than that during wetter conditions. This change in composition may indicate that the main source of baseflow changes with antecedent precipitation; relatively wet conditions enhance baseflow contribution from interflow, while drier conditions (which exhibit reduced interflow volume) result in a greater percentage of baseflow sourcing from saturated zone water. Actual values of ANC are comparable to those found by Cook et al. (1994) in a study of five GSMNP streams and by Carline et al. (1992) on Pennsylvania's Northern Appalachian Plateau, an area similar in topography, geology, and vegetation to the Ramsay Prong catchment. Flum and Nodvin (1995) reported the same pattern of increased ANC with lower elevation.

Values of pH exhibited consistent spatial variation and an unanticipated temporal pattern. In terms of location, pH climbed with decreasing elevation. This can be attributed to the low ANC in the higher altitudes as compared to the basin bottom; geology nearer to Ramsay Cascades does not facilitate buffering of stream water. This observation is common in basins throughout GSMNP (Silsbee and Larson 1982). Temporal trends are not as straight forward and may imply trends in GW-SW interactions. Despite some of the lowest pH values in August antecedent throughfall, the highest pH was seen in August. Similar throughfall pH was observed during March and April, but April baseflow is the most acidic. Furthermore, July, which displayed the highest pH in throughfall (see Appendix A) in addition to the highest volume of antecedent precipitation, was characterized by a pH in baseflow that closely resembled August baseflow. Two inferences can be made from these trends. First, August

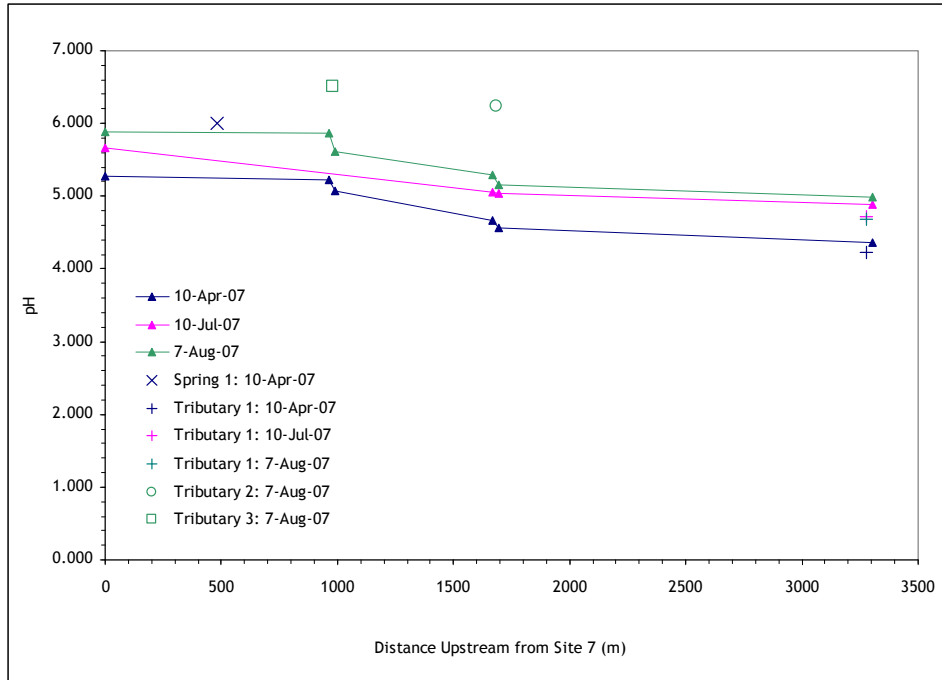


Figure 5. Measured pH values in Ramsay Prong, tributaries, and adjacent springs on each monitoring day (after Owen 2007).

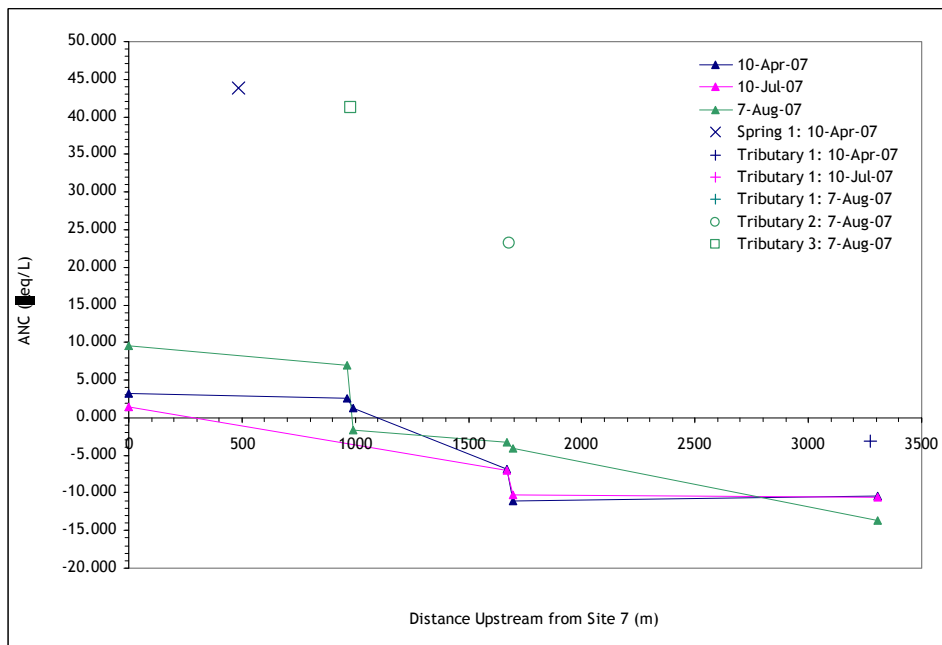


Figure 6. Measured ANC in Ramsay Prong, tributaries, and adjacent springs on each monitoring day (after Owen 2007).

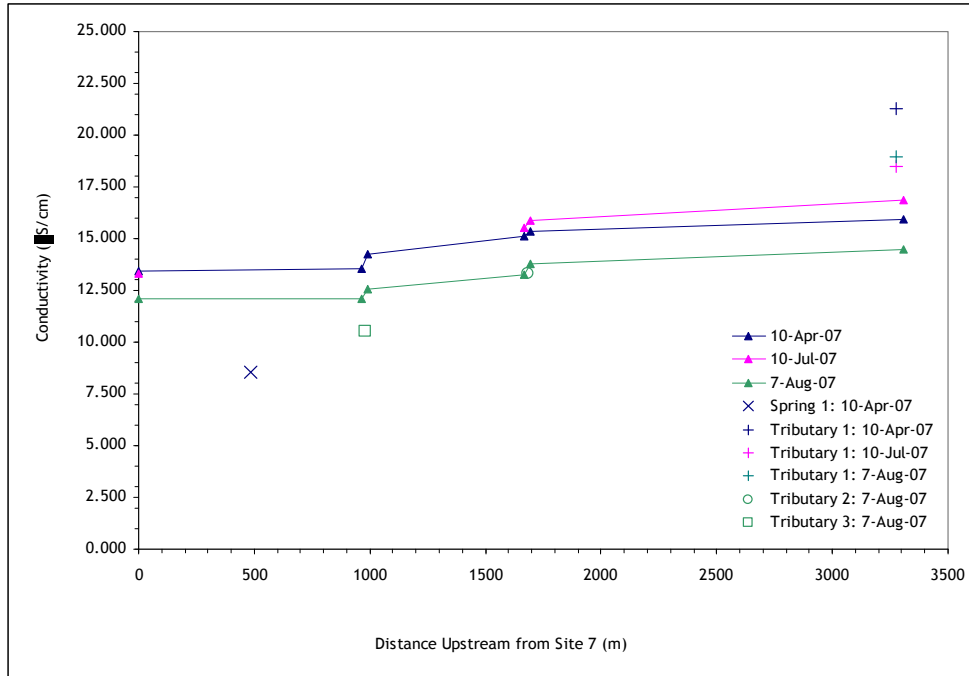


Figure 7. Measured conductivity in Ramsay Prong, tributaries, and adjacent springs on each monitoring day (after Owen 2007).

baseflow was supplied by a greater percentage of groundwater than that of April. Second, July baseflow did not source from groundwater to any substantial amount (because pH did not change from throughfall to streamwater). It is probably, then, that July and April baseflow was comprised of more interflow than in August, with July containing the most. The range of pH values recorded in this study is comparable to those found in other investigations of GSMNP (Silsbee and Larson 1982; Flum and Nodvin 1995; Nodvin et al. 1995; Neff 2007).

4.5.2 Dissolved Constituents

As previously mentioned, water samples from Ramsay Prong were analyzed for major ions, trace metals, and total silica. Figures 8 and 9 depict spatial concentration trends on each monitoring date for major ions and trace metals plus total silica; data used to draw these plots was originally reported in Owen (2007).

Due to approximately constant ionic concentrations, mass accretion rates for all species predominantly followed the pattern of discharge in Ramsay Prong; Figures 14 and 15 in Appendix A display these trends. However, some ions displayed variation in their magnitude both spatially and temporally. These fluctuations can be attributed to combinations of different weathering rates, mobility, biological uptake, and atmospheric deposition.

The most abundant minerals in Ramsay Prong basin can be listed in the following order of least to greatest resistance to weathering, as inferred from Berner and Berner (1987) and Appello and Postma (2005).

Dolomite < K-feldspar < Slate < Quartz < Kaolinite

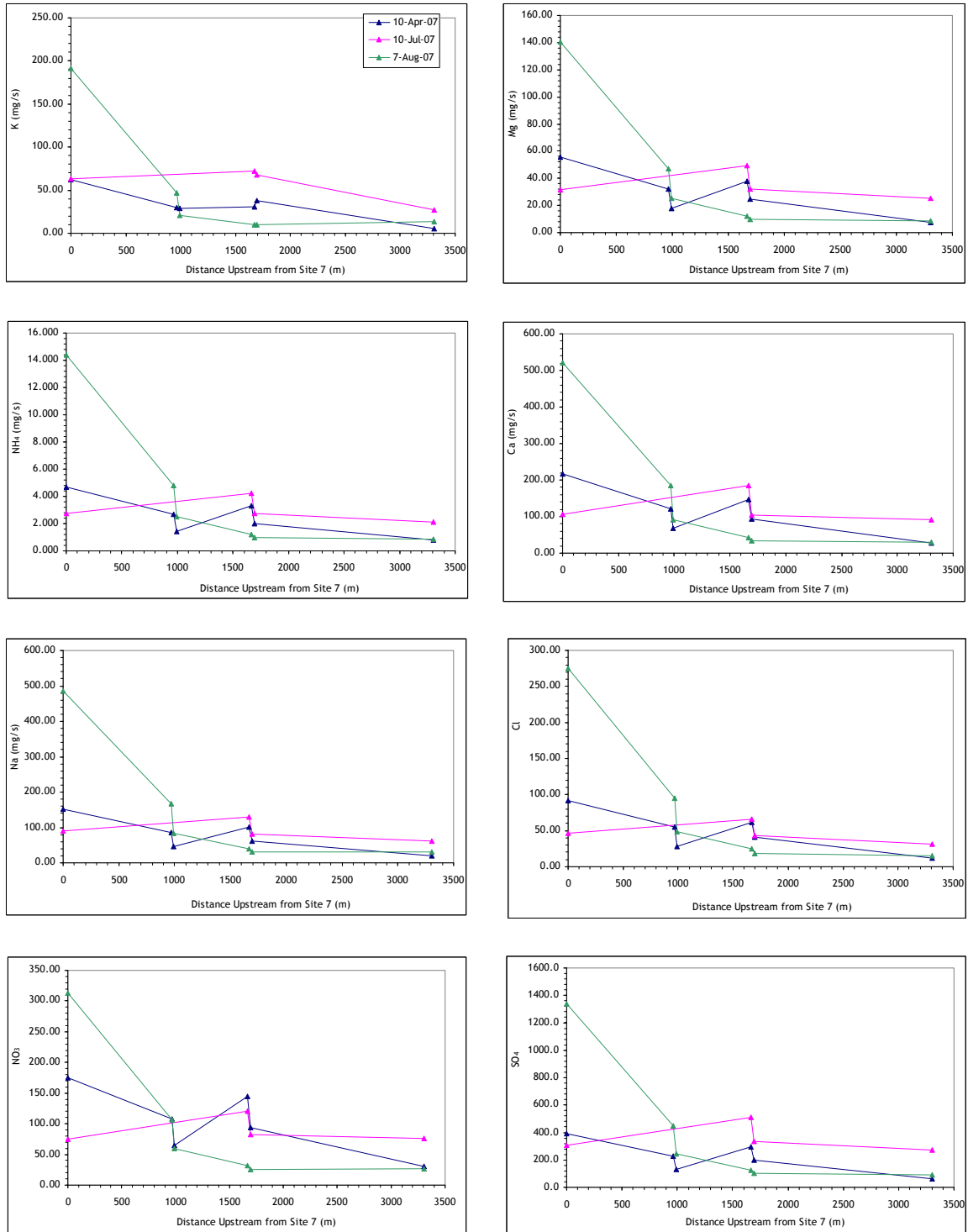


Figure 8. Concentration trends with distance upstream from Site 7 for major ions in Ramsay Prong, tributaries, and adjacent springs on each monitoring day (after Owen 2007).

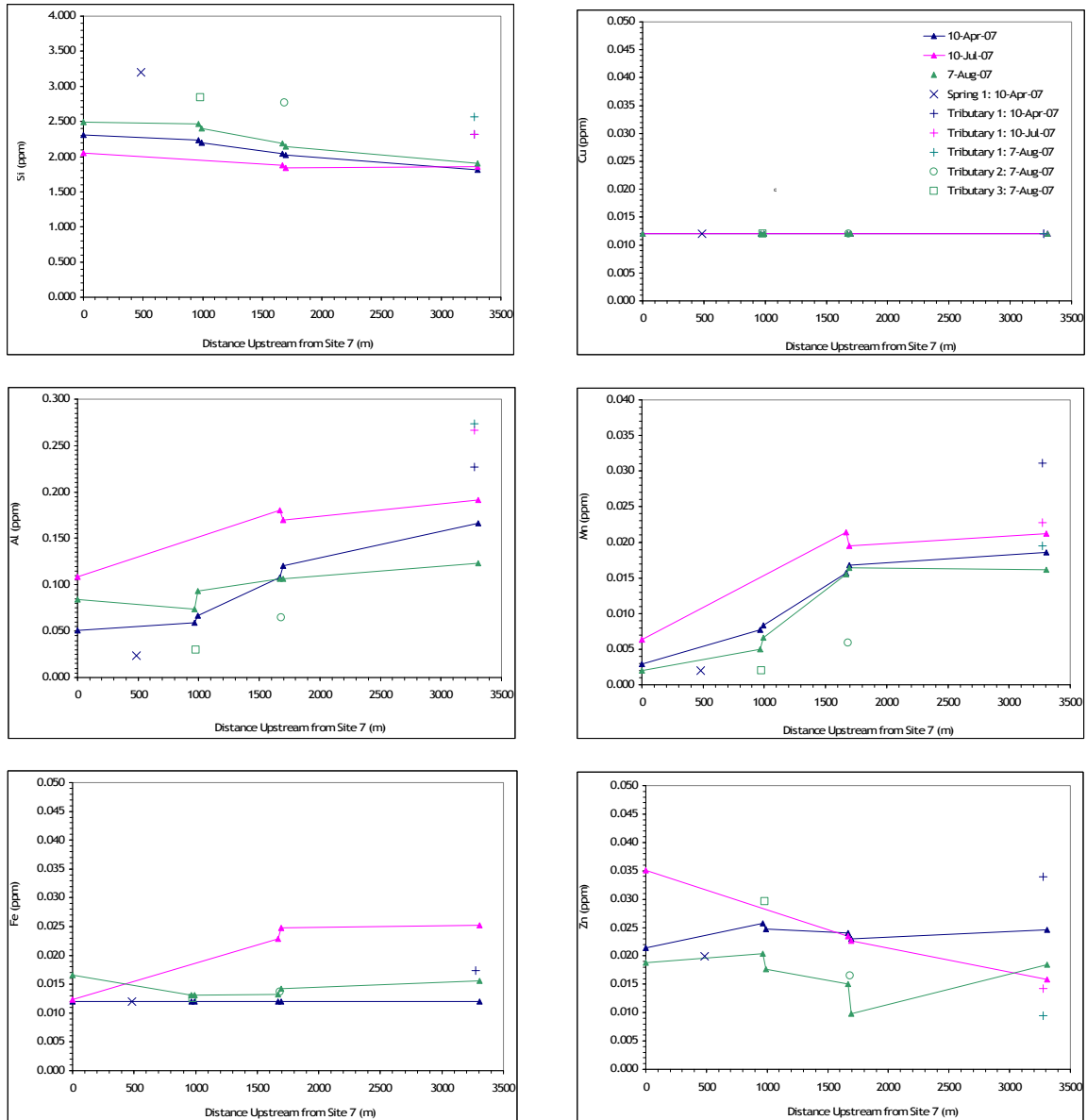


Figure 9. Concentration trends with distance upstream from Site 7 for trace metals and total silica in Ramsay Prong for each monitoring date (after Owen 2007).

Berner and Berner (1987) also point out the relative mobility of major dissolved species, stating that aluminum and iron tend to remain sorbed onto soil particles:

$$\text{Ca} \geq \text{Na} \geq \text{Mg} \geq \text{Si} \geq \text{K} \gg \text{Al} \approx \text{Fe}$$

Biological activity is also unequal for different nutrients. Defined as the ratio of an element stored annually in vegetation—living and dead—to the annual loss from the area in streamflow, comparative biological uptake of major ions are described by Berner and Berner (1987) in decreasing order:

$$\text{P} > \text{N} > \text{K} > \text{Ca} > \text{S} > \text{Mg} > \text{Na}$$

These three qualitative assessments are keys to understanding patterns of rock-water interactions along Ramsay Prong and ultimately describing GW-SW interactions in the basin.

4.5.2.1 Sulfate & Nitrate

According to Berner and Berner (1987), “clean” air in North America contains no more than 31 µeq/L (0.6 mg/L) of sulfate and less than 24 µeq/L (1.5 mg/L) of nitrate. The pollution of throughfall in Ramsay Prong basin is thus evident (see Appendix A), and the large concentrations of sulfate and nitrate in baseflow are unsurprising. Furthermore, the increase in these species with additional antecedent rainwater was also expected as a greater mass of acidic inputs entered the system. In the same respect, higher headwater concentrations of nitrate and sulfate were anticipated as precipitation typically increases with elevation in mountainous terrain (Wilson and Guan 2004).

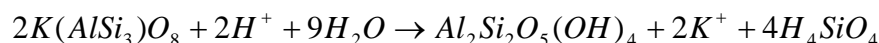
Sulfate can also source from slate dissolution and subsequent oxidation of iron sulfides (e.g., pyrite), but the unusually high rate of anthropogenic sulfate deposition most likely masks this effect, if it occurs at all. However, despite the substantial source via precipitation, sulfate measured in Ramsay Prong is particularly low when compared to literature values. This is not an uncommon field observation, though, as Berner and Berner (1987) explain, and has been attributed to bacterial reduction of sulfate to hydrogen sulfide (H₂S) and sorption onto soil particles.

Besides atmospheric deposition, nitrate is produced by nitrification of ammonium. Since manure is the chief source of ammonium, it is most probable that acid rain is the supplier of nitrate in this case. The spatial and temporal distributions, as described above, bolster this theory.

4.5.2.2 Potassium Feldspar Weathering

Since the bedrock in Ramsay Prong has been identified as potassium feldspar, concentrations of potassium, aluminum, and silica will reveal areas where the source of baseflow has greatest interaction with either the clay saprolite (kaolinite) or the bedrock itself.

As noted by Appelo and Postma (2005), weathering of K-feldspar is relatively difficult as it dissolution is controlled by surface processes and not transport. Nesbitt et al. (1997) report its leach rate to be on the order of 10⁻¹¹ to 10⁻¹² mol·m⁻²·sec⁻¹ under ambient temperature and pressure at pH 5; a decrease in pH to 3.5 can raise the dissolution by an order of magnitude. This weathering reaction releases potassium ions, leaving behind kaolinite clay [Al₂Si₂O₅(OH)₄], as seen in the equation below.

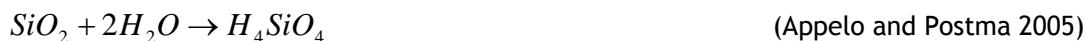


(Appelo and Postma 2005)

The second step releases aluminum ions and silicic acid [H₄SiO₄], as shown below.



Silica is also released by quartz weathering according to a dissolution rate on the order of 10⁻¹³ mol·m⁻²·sec⁻¹ under ambient temperature and pressure with pH less than 6 (Nesbitt et al. 1997; Appelo and Postma 2005). This reaction generates silica in the form of silicic acid, as demonstrated below.



Typically, fresh water contains 0.56-28mg/L of Si (Appelo and Postma 2005), a range in which Ramsay Prong falls at the low end with approximately 1.8-3.2mg/L of Si. This was expected because sedimentary silicates (i.e., sandstone) are more resistant to erosion than igneous and metamorphic silicates due to the relatively large composition of detrital minerals, particularly quartz and clay in this case, that are essentially unable to be weathered. Other GSMNP investigations have gleaned similar results; Cook et al. (1994) observed a range of 0.5-1.4mg/L, while Silsbee and Larson (1982) measured a band of approximately 2-5mg/L. Nevertheless, silica concentrations in Ramsay Prong slightly increased both temporally and spatially from the top to the bottom of the channel. The temporal trend can be attributed to the increasing contribution of groundwater to baseflow with less antecedent precipitation. Due to the small amount of silica found in throughfall, a slight concentration jump was observed in the headwaters in July. However, this addition did not reach the magnitude of August, indicating that groundwater is the main source of silica in Ramsay Prong. The spatial fluctuation also bolsters this suggestion as the rise in silica loading rate reveals the existence of long groundwater flowpaths moving down the basin; longer contact with the saprolite results in greater accumulation of dissolved silica.

Potassium is found in fresh water at approximately 0.39-7.8mg/L (Appelo and Postma 2005), but Ramsay Prong exhibited concentrations in the range of 4.2-12.5mg/L. Other GSMNP streams have been recorded to contain approximately 0.5-2.0mg/L K (Silsbee and Larson 1982; Cook et al. 1994). Ramsay Prong's high-end values may be representative of the large volume of K-feldspar throughout the basin but are more likely caused by antecedent precipitation. Chemical analysis of throughfall illustrates that the basin was subjected to a mass of potassium several times larger than stream measurements. However, since potassium in the stream was much less than in precipitation, potassium must have been taken up by vegetation prior to reaching the channel. Moreover, because potassium concentrations accreted only with sufficient antecedent precipitation, it is apparent that a flushing mechanism had been activated in the headwaters; relatively old water was replaced by younger interflow. Presuming that during drought conditions, baseflow in the headwaters was well-dominated by groundwater, observations of declining potassium loading rates (when moving downslope from Ramsay Cascades) in August indicate that potassium did not source from storage in the high elevations. However, the relatively large jump in accretion at the basin bottom is characteristic of long flowpaths through the bedrock. Measurements of April baseflow—which was a mixture of interflow and groundwater—support this theory; the smaller recovery of potassium at the basin bottom denotes some contribution from groundwater.

Precipitation provides a small amount of aluminum to the basin, but because the concentration of this metal in the stream water is equally low, much of the aluminum in Ramsay Prong can be attributed to this atmospheric deposition. Additionally, inferences concerning the source of baseflow can be made based upon aluminum's spatial and temporal fluctuations in the channel. While aluminum content steadily decreased from the top to the bottom of the catchment, its magnitude varied by date. The macroscopic spatial pattern indicates a constant source of

aluminum in the high elevations with little to no addition moving down the channel. Coupled with temporal observations, it is evident that the principle aluminum inputs are from precipitation. However, based on August aluminum measurements at S6 and S7, some aluminum does source from baseflow. The rise in concentration at the basin bottom is indicative of a large contribution of groundwater that has traveled long flowpaths in contact with kaolinite. In contrast, the recovery of aluminum was not seen at the same magnitude in April because a smaller portion of baseflow sourced from groundwater.

4.5.2.3 Other Species

The remaining measured species (i.e., Ca, Mg, Na, NH_4 , Cl, Cu, Zn, Fe, and Mn) exhibited relatively stable concentrations on a global basis. Some constituents did display somewhat erratic behavior between the monitoring sites, but these variations are simply indicative of local geology and residence times. For instance, the marked rise in Ca and Mg between S6-S7 in August is validation that long flow pathways exist in the basin; Ca and Mg source mainly from dolomite in the sandstone. Furthermore, the consistent jump in loading rates of all species over this reach in August and April imply that the area is able to capture and retain water from both interflow and subsurface fluxes.

4.5.2.4 Comparative Studies

A year-long study across basins in GSMNP, including Ramsay Prong, by Silsbee and Larson (1982) found similar trends in dissolved constituents. In particular, Si, K, and Na fell with increasing elevation, while the opposite is true for nitrate. Calcium and magnesium showed no apparent patterns. Furthermore, Silsbee and Larson (1982) agree that lower elevation areas exhibit longer groundwater retention and thus contain a greater amount of geologically-derived species.

4.6 Stable Isotopes

4.6.1 Results and Influences

Oxygen ($\delta^{18}\text{O}$) and hydrogen ($\delta^2\text{H}$) isotopes in the streams, tributaries, and spring are presented via three approaches in Figures 10 through 12. The first presents the data linearized by monitoring site to illustrate a spatial systemic mean; the second portrays the systemic differences on a temporal basis; the third compares the temporal variations by site.

Deuterium and O-18 measurements are interpreted by comparison of a single investigation's data with the meteoric water line (MWL). By definition, the MWL is a plot of average O-18 concentration (x-axis) versus deuterium concentration (y-axis) in precipitation. Comparisons are performed between slopes as well as in terms of location on the graph (i.e., does the data sit above or below the MWL?). In effect, deviations from the MWL are indicative of specific processes that the water has undergone after falling as precipitation. A MWL has been developed for the globe, but some have also been reported for specific areas. Implementation of a local MWL is ideal for a study that is relatively localized, such as this one, as it allows direct comparison of precipitation and stream water. However, the global MWL can also be used when a local trend has not been established. In this case, it is important to consider large-scale properties of the location, particularly latitude and distance from the coast, as precipitation isotopic composition varies predictably with these factors.

A local MWL does not exist for this area, so the global MWL found by the United Nations International Atomic Energy Agency (IAEA), as described by Hoefs (2004), is utilized. Compared to literature values for global precipitation (Clark and Fritz 1997), the data collected in this study reflects a typical meteoric relationship for global precipitation in warm regions.

Deuterium enrichment can be caused by three factors: rock-water interactions, evaporation, and exchange with hydrogen sulfide (H₂S). However, the latter reaction is an extremely rare natural occurrence (Clark and Fritz 1997) and is not considered a viable explanation for deuterium enrichment in this investigation. The enrichment is therefore attributed to evaporation in the basin and rock-water exchanges.

Similar to deuterium, oxygen-18 fractionation is controlled by evaporation and rock-water interactions. Evaporative mechanisms result in enrichment, while exchanges between minerals generate depleted conditions as O-18 tends to partition to the solid phase. Relevant interactions for O-18 in stored groundwater of Ramsay Prong include those with quartz (SiO₂), potassium feldspar, clay hydration waters, or carbonate (CO₂) (Clark and Fritz 1997). However, the carbonate fractionation reaction is atypical in nature, and isotope exchange with quartz (SiO₂) occurs only at high temperatures (i.e., >100°C) (Clark and Fritz 1997). Besides evaporation, the only probable explanations for O-18 concentration changes here are, therefore, interactions with K-feldspar and kaolinite hydration waters. Table 2 presents the reactions between minerals and stable oxygen and hydrogen isotopes.

4.6.2 Systemic Patterns

Figure 10 shows that on average the basin is isotopically similar on a spatial basis. In particular, the mean trend at all sites portrays a system that is enriched in either deuterium, depleted in O-18, or both. The first explanation implies high evaporation rates, the second points to substantial rock-water exchanges, and the third suggests a mixture of the two.

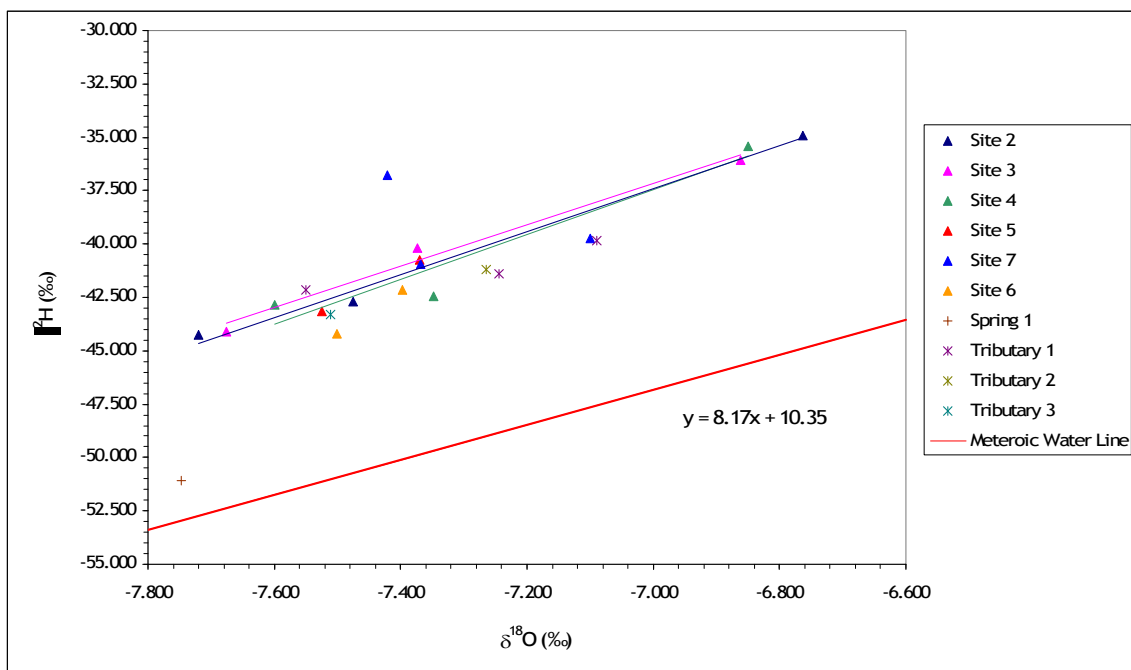


Figure 10. Spatial relationship between deuterium and O-18 in Ramsay Prong, tributaries, and adjacent springs aggregated by location.

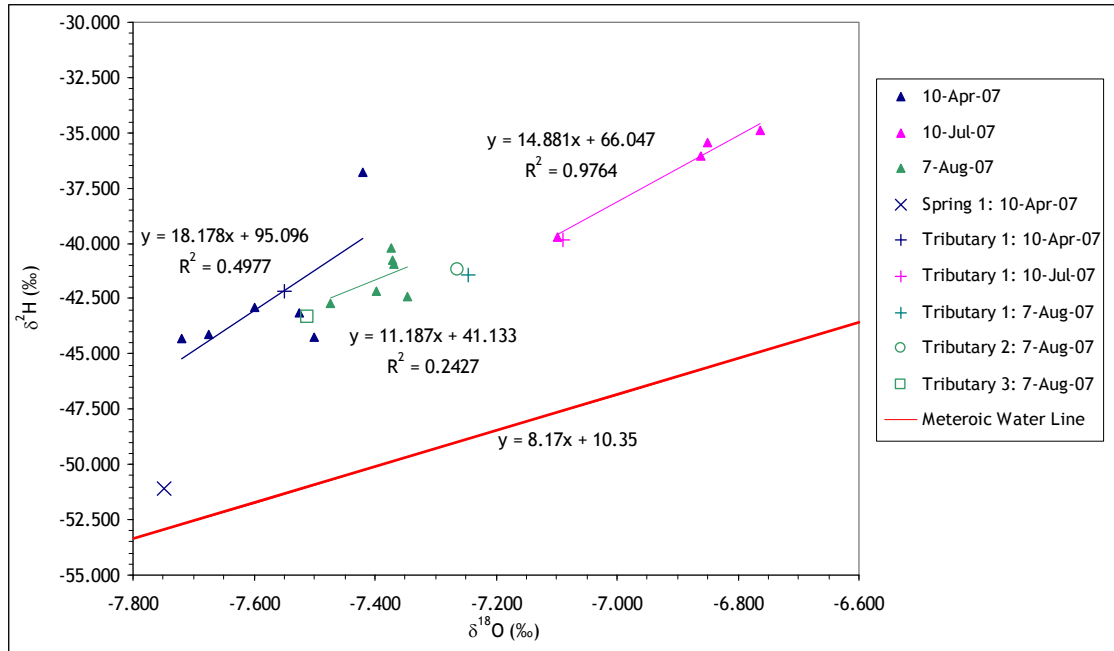


Figure 11. Temporal relationships between deuterium and O-18 in Ramsay Prong, tributaries, and adjacent springs aggregated by date.

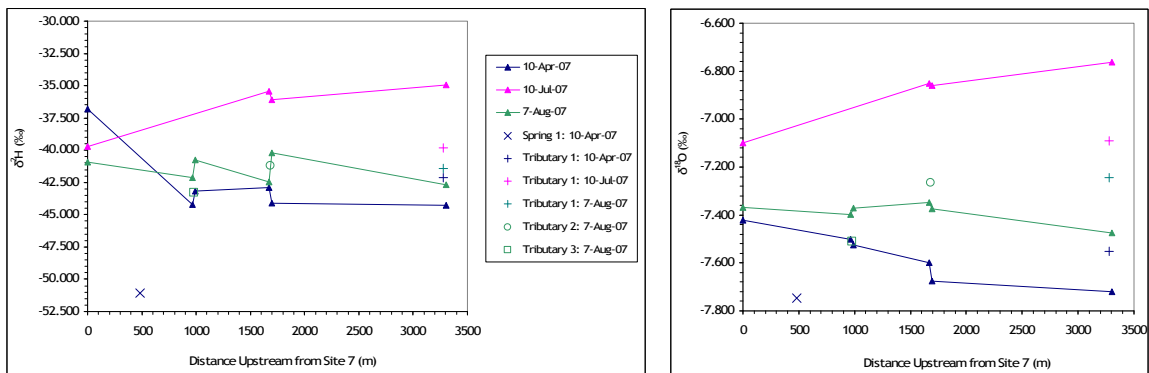


Figure 12. Deuterium and O-18 patterns with distance upstream from S7 for each monitoring date.

Table 2. Potential water-rock exchange reactions for ^2H and ^{18}O in Ramsay Prong basin.

<i>Mineral</i>	<i>Isotope Exchange Reaction</i>	<i>Reference</i>
K-Feldspar	$K\text{AlSi}_3\text{O}_7^{18}\text{O} + \text{H}_2\text{O} \leftrightarrow K\text{AlSi}_3\text{O}_8 + \text{H}_2^{18}\text{O}$	Clark and Fritz 1997
Weathered Clay Hydration Waters	$\text{Al}_2\text{Si}_2\text{O}_5(\text{OH})_3(^{18}\text{OH}) + \text{H}_2\text{O} \leftrightarrow \text{Al}_2\text{Si}_2\text{O}_5(\text{OH})_4 + \text{H}_2^{18}\text{O}$ $\text{Al}_2\text{Si}_2\text{O}_5(\text{OH})_3(\text{O}^2\text{H}) + \text{H}_2\text{O} \leftrightarrow \text{Al}_2\text{Si}_2\text{O}_5(\text{OH})_4 + \text{H}^2\text{HO}$	Clark and Fritz 1997; Appelo and Postman 2005

It is impossible to determine the exact situation because a local meteoric water line does not exist. However, the trend lines do portray a deuterium excess (i.e., y-intercept) of approximately 30‰, the typical value for this latitude (SAHRA 2005), indicating that the isotopes do reflect a relationship that is expected for the region.

4.6.3 Temporal Patterns

The second isotope plot, Figure 11, illustrates the temporal relationship, specifically the source of baseflow with sampling date. Most apparent is the observation that July experienced more enrichment in both deuterium and O-18 than either the early spring or late summer date. This may be due to a difference in temperature during storm events; warmer temperature induces greater fractionation and thus more enriched precipitation (Clark and Fritz 1997; SAHRA 2005). Although this could explain the relative depletion in April, August likely experienced similar temperatures as July. Therefore, a second mechanism was in affect—evaporation. July baseflow was most likely dominated by shallowly stored interflow such that, prior to becoming baseflow, it was subjected to evaporative mechanisms to a greater extent than the baseflow source water in August (and April). In essence, July's antecedent precipitation had replaced a large amount of this shallow storage, flushing it out as baseflow. This replacement of "old" water with "new" water in the saturated and near-saturated zones has also been detected through tracer experiments in the Cairngorms region of Scotland (Soulsby et al. 2000). In fact, the storm hydrograph was dominated by the older isotopic character, indicating that precipitation from the recent storm event had remained in the subsurface.

Another important point to confirm baseflow source is the deuterium excess in April indicates that the sampled water did not source from snowpack (at any significant level); if it had, deuterium depletion would have been observed, particularly in April.

4.6.4 Spatial Patterns

Spatial variations in isotopic concentrations are visible in Figure 12. Most apparent is the transition from a larger range of concentrations in the higher elevations to a narrower range in the lower altitudes. This trend indicates a greater degree of GW-SW interaction with movement toward the basin bottom. In effect, the convergence of these values illustrates that mixing occurs as water travels to the lower part of the catchment where baseflow becomes more reflective of the mean groundwater character.

Figure 12 also characterizes the baseflow sources within subbasins. As Hoefs (2004) describes, isotopic dissimilarities between precipitation and groundwater recharge are caused by (1) recharge from surface water bodies that are partly evaporated, (2) recharge exhibiting variant isotopic composition due to its generation during a different climatic period, and (3) isotopic fractionation induced by interactions with soil, the aquifer, or geologic formations. Any of these three mechanisms could play a role in Ramsay Prong basin, but further investigations to specifically sample groundwater and precipitation are warranted. Results from this study can speak only on a qualitative basis regarding streamflow.

Baseflow is indeed affected by the rate of evaporation across the catchment, but isotopic fluctuations within the subbasins are also indicative of reactions with the bedrock and kaolinite. In the case of O-18, if the partitioning is relatively small, the effect may be mitigated by the magnitude of evaporation, while with regard to deuterium, if the partitioning is large, the result would be enhanced by evaporation. As a result, interaction with bedrock and possibly kaolinite is identified by simultaneous enrichment of deuterium and dampening or stabilization of O-18. Reach S6-S7 as well as T2 may be incurring this situation in August as a substantial enrichment in deuterium is accompanied by a meager enrichment in O-18. Additionally, the opposite signs in slopes of deuterium and O-18 concentrations between S4 and S5 in August clearly point to exchange between the rock-water interface. These trends suggest, as before, that the lower portions of the basin receive a greater contribution to baseflow from groundwater stored in contact with the bedrock. Furthermore, as these patterns are only observed in August, this month must have incurred the largest percentage of groundwater in baseflow.

5. Discussion

5.1 Drought Implications

During the course of this study, drought decreased the hydraulic head during baseflow across the Ramsay Prong basin. The amount of groundwater in storage (and thus comprising baseflow) was reduced, and, in effect, the observed discharge is low baseflow. However, as stated previously, decades to centuries of climate change are necessary for permanent modifications in the GW-SW relationship. Therefore, trends in GW-SW interactions cannot have been altered, yet, as the drought has persisted for an inadequate duration of time. It is thus assumed in this discussion that observations during the investigation reflect typical qualitative exchanges between groundwater and surface water in Ramsay Prong basin.

5.2 Conceptual Model

The observed trends in geology, topography, geochemistry, and climate are indicative of a system exhibiting diffuse groundwater recharge with little storage in the high elevations and focused recharge with relatively large storage in the lower elevations. Interflow is directed downhill by a relatively thin layer of weathered rock and soil that appears largely confined by an underlying low permeability bedrock unit. However, a shallow fracture system in the sandstone bedrock may exist, funneling groundwater to the lower elevations. In effect, the system acts as a slowly draining tank, temporally cycling between refill and release periods at the bottom of the basin. Additionally, areas of bedrock depressions may exist that hinder baseflow supply during low flow conditions. However, this also leads to increased residence time such that increased mineral dissolution occurs. A conceptual diagram of the Ramsay Prong basin is shown in Figure 13.

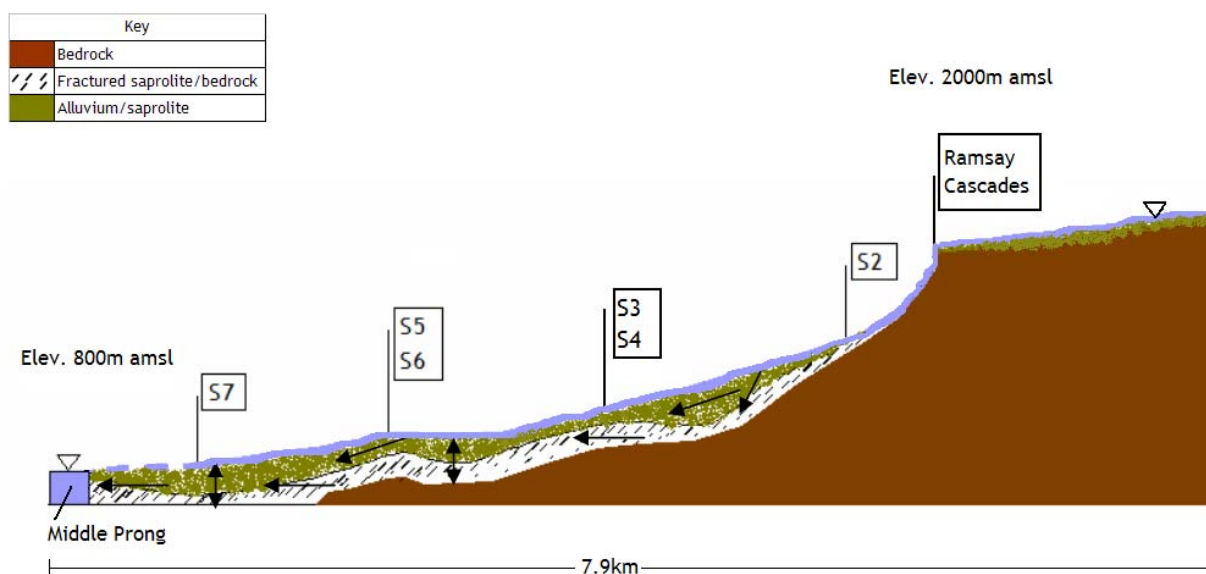


Figure 13. Conceptual diagram of the flow pathways in Ramsay Prong basin below Ramsay Cascades.

A mixture of shallow groundwater storage and interflow is the main contributor to baseflow in Ramsay Prong climate. During periods of abundant precipitation, interflow makes up the greatest percentage of baseflow, while durations that experience a lower amount of precipitation generate baseflow from groundwater storage. In turn, drought conditions require that nearly all baseflow sources from storage in the saturated zone (Smakhtin 2001). Brunke and Gonser (1997) found this behavior typical for regional GW-SW exchanges.

Fracture networks may play a role in supplying baseflow from these aforementioned shallow storage areas. A large network extending throughout the basin or small pockets of fractures may capture and supply water to the channel; both saprolite and bedrock fractures likely exist. However, due to the predominantly consistent geochemistry in the catchment, these networks—if they exist—are disconnected from deep aquifer storage. (If connection to deep storage did exist, baseflow would have been better maintained.) Nevertheless, these networks are the catalysts of long flow paths throughout the basin.

Streamflow losses along Ramsay Prong appear to be caused by two different mechanisms: evaporation and downward fluxes through the alluvium. Such an observation was anticipated as these losses are fundamentally characteristic of mountainous terrain, particularly in the low elevations (Fetter 2001; Bartolino and Cole 2002). Moreover, Ramsay Prong may exhibit substantial bedrock depressions, particularly between S4 and S5. Once filled, these bowls sustain baseflow in the lower altitudes of the basin. It is important to note that higher altitudes did not exhibit streamflow loss, even with endured drought. Based on observations in slope and soil cover in these areas, it is likely that the principal source of water is somewhere above the cascades and not within the higher reaches.

5.3 Ecological Implications

Ramsay Prong basin does not exhibit the characteristics needed to withstand continued acid deposition, especially if global warming (and reduced precipitation) persists. As reflected by the low ANC values and high acid composition, this is not a well-buffered system. Such sensitivity in high-altitude catchments appears to be common in GSMNP. Nodvin et al. (1995) found the same situation in nearby Noland Divide, noting pH values under 6 and ANC below 40 μ eq/L, and Cook et al. (1994) reported values not exceeding 6.4 for pH and 28 μ eq/L for ANC. However, as evidenced by the relatively higher concentrations of aluminum in the headwaters, some neutralization power does exist via the dissolution of K-feldspar and kaolinite.

The sensitivity of Ramsay Prong to acid deposition has notable ecological implications. In particular, less-hardy fish species, such as native brook trout, may be eradicated from the stream, particularly in the high elevation reaches. Only the very bottom of the basin may prove suitable for these sensitive fauna. In fact, Neff (2007) reported that only 0.2-km of Ramsay Prong at or below an elevation of 821m currently supports brook trout, whereas 1.0km was supportive at up to 914m in 1985 (Bivens et al. 1985). It is evident that the low buffering capability of Ramsay Prong basin will result in habitat depletion for certain fish species if acidic inputs are not mitigated.

The onset of global warming warrants predictions for continued drought conditions. Should precipitation continue to wane, baseflow will eventually be depleted. Ramsay Prong catchment does not have the ability to store water at the higher elevations, and storage at its base is limited. Persisting temperature increases with reduced precipitation will undoubtedly dry the basin from the top down, resulting in aquatic and terrestrial ecosystem losses.

6. Conclusions

This study presents a methodology for evaluating GW-SW patterns in areas where data collection is limited due to a remote location and legal protection. Hydrologic, geochemical, and isotopic parameters are measured on three dates at six key points along a main channel in GSMNP. Inferences from this data encompass the following:

1. Poor soil cover, steep slopes, and low permeability bedrock result in a storage capacity that is insufficient to supply typical baseflow volume in the headwaters during extended dry periods;
2. Baseflow is supplied by interflow as well as shallow groundwater storage. The portion of baseflow comprised by interflow increases with increasing antecedent precipitation.
3. A shallow fracture network likely provides long flowpaths for water to travel toward the basin bottom.
4. Diffuse groundwater recharge occurs mainly in the headwaters where steep slopes dominate the topography, while focused recharge occurs in bedrock depressions and at the end of the channel.
5. Acid neutralization is best facilitated at the bottom of the catchment where sufficient alluvium exists to capture and recharge the basin water supply.

This study was constructed as an initial investigation of Ramsay Prong basin and, as such, could generate only a general characterization of the catchment. It is recommended that further probing be performed to validate and improve the conclusions of this research. Such ventures should include: frequent and routine discharge measurements along the main channel; discharge measurements of the tributaries; spatial identification and additional geochemical and isotopic characterization of major springs; soil classification throughout the basin; and monitoring of precipitation volume and chemistry throughout the catchment. Ecosystem health should also be reviewed as continued acid deposition without sufficient groundwater recharge will likely propagate environmental damage.

Despite the challenges with conducting field investigations in remote and legally protected areas, this study has shown the importance of continuing such efforts in order to better understand and guard these undisturbed areas.

References

- Appelo, C.A.J., and D. Postma. 2005. *Geochemistry, Groundwater and Pollution*. 2nd ed. New York: A.A. Balkema Publishers.
- Bartolino, J.R., and J.C. Cole. 2002. Ground-water resources of the Middle Rio Grande basin. USGS Circular 1222.
- Berkowitz, B. 2002. Characterizing flow and transport in fractured geologic media: a review. *Advances in Water Resources* 25: 861-884.
- Berner, E.K., and R.A. Berner. 1987. *The Global Water Cycle: Geochemistry and Environment*. Englewood Cliffs, New Jersey: Prentice Hall, Inc.
- Bivens, R.D., Stranger, R.J., and D.C. Peterson. 1985. Current distribution of the native brook trout in the Appalachian region of Tennessee. *Journal of the Tennessee Academy of Science* 60: 4, 101-105.
- Boulton, A.J., and P.J. Hancock. 2006. Rivers as groundwater-dependent ecosystems: a review of degrees of dependency, riverine processes and management implications. *Australian Journal of Botany* 54: 133-144.
- Brunke, M. and T. Gonser. 1997. The ecologic significance on exchange processes between rivers and groundwater. *Freshwater Biology* 37: 1-33.
- Buchanan, T.J., and W.P. Somers. 1976. Discharge measurements at gaging stations. *Techniques of Water-Resource Investigation of the United States Geological Survey* Book 3. Chapter A8. Washington: United States Government Printing Office.
- Buttle, J.M., Dillon, P.J., and G.R. Eerkes. 2003. Hydrologic coupling of slopes, riparian zones, and streams: an example from the Canadian Shield. *Journal of Hydrology* 287: 161-177.
- Carline, R.F., DeWalle, D.R., Sharp, W.E., Dempsey, B.A., Gagen, C.J., and B. Swistock. 1992. Water chemistry and fish community responses to episodic stream acidification in Pennsylvania, USA. *Environmental Pollution* 78: 45-48.
- Clark, I., and P. Fritz. 1997. *Environmental Isotopes in Hydrogeology*. New York: CRC Press LLC.
- Eaton, T.T. 2006. On the importance of geological heterogeneity for flow simulation. *Sedimentary Geology* 184: 187-201.
- Fetter, C.W. 2001. *Applied Hydrogeology*. 4th ed. Upper Saddle River, New Jersey: Prentice Hall, Inc.
- Flum, T., and S.C. Nodvin. 1995. Factors affecting stream water chemistry in the Great Smoky Mountains, USA. *Water, Air and Soil Pollution* 85: 1707-1712.
- Freeze, R.A., and P.A. Witherspoon. 1967. Theoretical Analysis of Regional Groundwater Flow 2. Effect of Water-Table Configuration and Subsurface Permeability Variation. *Water Resources Research* 3: 623-634.
- Hoefs, J. 2004. *Stable Isotope Geochemistry*. 5th ed. New York: Springer.
- Lindberg, S.E., and G.M. Lovett. 1992. Deposition and forest canopy interactions of airborne sulfur—results from the Integrated Forest Study. *Atmospheric Environment* 26A: 1477-1492.
- Mayer, J.R., and J.M. Sharp. 1998. Fracture control of regional ground-water flow in a carbonate aquifer in a semi-arid region. *Geological Society of America Bulletin* 11, no. 2: 269-283.
- Mitchell-Bruker, S., and H.M. Haitjema. 1996. Modeling steady-state conjunctive groundwater and surface water flow with analytic elements. *Water Resources Research* 32: 2725-2732.
- Moore, H.L. 1995. *A Roadside Guide to the Geology of the Great Smoky Mountains National Park*. Knoxville, TN: The University of Tennessee Press.
- Morrice, J.A., Valett, H.M., Dahm, C.D., and M.E. Campana. 1997. Alluvial characteristics, groundwater-surface water exchange and hydrological retention in headwater streams. *Hydrological Processes* 11: 253-267.
- National Drought Mitigation Center. 2007. U.S. Drought Monitor. University of Nebraska—Lincoln. http://www.drought.unl.edu/dm/DM_state.htm?TN,S (accessed 10 August 2007).

- National Park Service. 2006. Great Smoky Mountains: Weather. U.S. Department of the Interior. <http://www.nps.gov/grsm/planyourvisit/weather.htm> (accessed 6 August 2007).
- National Research Council. 2004. *Groundwater fluxes across interfaces*. National Academy Press: Washington, D.C.
- Nastev, M., Savard, M.M., Lapcevic, P., Lefebvre, R. and R. Martel. 2004. Hydraulic properties in scale effects investigation in regional rock aquifers, south-western Quebec, Canada. *Hydrogeology Journal* 12: 257-269.
- Neff, K. 2007. In situ bioassays of native brook trout (*salvelinus fontinalis*) in streams affected by episodic acidification in the Great Smoky Mountains National Park. Master's Thesis, The University of Tennessee—Knoxville.
- Nesbitt, H.W, Fedo, C.M., and G.M. Young. 1997. Quartz and feldspar stability, steady and non-steady state weathering, and petrogenesis of siliciclastic sands and muds. *The Journal of Geology* 105: 173-191.
- Nodvin, S.C., Van Miegroet, H., Lindberg, S.E., Nicholas, N.S., and D. W. Johnson. 1995. Acid deposition, ecosystem processes, and nitrogen saturation in a high elevation southern Appalachian watershed. *Water, Air and Soil Pollution* 85: 1647-1652.
- Owen, C. 2007. Using multivariate analysis of geochemical data to better define hydrologi interfaces in surface water-groundwater systems. Master's Thesis. The University of Tennessee—Knoxville.
- Oxtobee, J.P.A., and K.S. Novakowski. 2003. Groundwater/surface water interaction in a fractured rock aquifer. *Ground Water* 41, no. 5:667-682.
- Power, G., Brown, R.S., and J.G. Imhof. 1999. Groundwater and fish - insights from northern North America. *Hydrological Processes* 13: 401-422.
- SAHRA. 2005. Isotopes and Hydrology. The University of Arizona. <http://www.sahra.arizona.edu/programs/isotopes/oxygen.html> (accessed 5 May 2007).
- Shubzda, J., Lindberg, S.E., Garten, C.T., and S.C. Nodvin. 1995. Elevations trends in the fluxes of sulphur and nitrogen in throughfall in the Southern Appalachian Mountains: some surprising results. *Water Air and Soil Pollution* 85: 2265-2270.
- Silsbee, D.G., and G. L. Larson. 1982. Water quality of streams in the Great Smoky Mountains National Park. *Hydrobiologia* 82, no. 2: 97-115.
- Silvapalan, M. 2003. Process complexity at hillslope scale, process simplicity at the watershed scale: is there a connection? *Hydrological Processes* 17: 1037-1041.
- Smakhtin, V.U. 2001. Low flow hydrology: a review. *Journal of Hydrology* 240: 147-186.
- Soil Data Mart. 2007. Natural Resources Conversation Service. U.S. Department of Agriculture. <http://soildatamart.nrcs.usda.gov>.
- Sophocleous, M., 2002. Interactions between groundwater and surface water: the state of the science. *Hydrogeology Journal* 10, DOI 10.1007/s10040-001-0170-8.
- Soulsby, C., Malcolm, A., Helliwell, R., Ferrier, R.C., and A. Jenkins. 2000. Isotope hydrology of the Allt a' Mharcaidh catchment, Cairngorms, Scotland: implications for hydrological pathways and residence times. *Hydrological Processes* 14: 747-762.
- Soulsby, C., Malcolm, A., Youngson, A.F., Tetzlaff, D., Gibbins, C.N., and D. M. Hannah. 2005. Groundwater-surface water interactions in upland Scottish rivers: hydrological, hydrochemical, and ecological implications. *Scottish Journal of Geology* 41: 39-49.
- Southworth, S., Schultz, A., and D. Denenny. 2005. *Geologic map of the Great Smoky Mountains National Park Region, Tennessee and North Carolina*. Open-File Report 2005-1225. U.S. Geological Survey, Denver, Colorado.
- Tóth, J., 1963. A theoretical analysis of groundwater flow in small drainage basins. *Journal of Geophysical Research* 68: 4785-4812.
- Tromp-van Meerveld, H.J., and J.J. McDonnell. 2006a. Threshold relations in subsurface stormflow: 1. A 147-storm analysis of the Panola hillslope. *Water Resources Research* 42, W02410, DOI 10.1029/2004WR00377
- Tromp-van Meerveld, H.J., and J.J. McDonnell. 2006b. Threshold relations in subsurface stormflow: 2. The fill and spill hypothesis. *Water Resources Research* 42, W02411, DOI 10.1029/2004WR003800.

- Vidon, P.G.F., and A.R. Hill. 2004. Landscape controls on the hydrology of stream riparian zones. *Journal of Hydrology* 292: 210-228.
- Warren, D. R., Sebestyen, S.D., Josephson, D.C., Lepak, J.M., and C.E. Kraft. 2005. Acidic discharge and in situ egg survival in redds of lake-spawning brook trout. *Transactions of American Fisheries Society* 134: 1193-1201.
- Wilson, J.L., and H. Guan. 2004. Mountain-block hydrology and mountain-front recharge. In *Groundwater recharge in a desert environment: The southwestern United States*, ed. J.F. Hogan, F.M. Phillips, and B.R. Scanlon, 113-138. Washington, D.C.: American Geophysical Union.
- Winter, T.C. 1995. Recent advances in understanding the interaction of groundwater and surface water. Supplement. *Reviews of Geophysics* 33: 985-994.
- Winter, T.C. 1999. Relation of streams, lakes, and wetlands to groundwater flow systems. *Hydrogeology Journal* 7: 28-45.
- Winter, T.C., Harvey, J.W., Frank, O.L., and W.M. Alley. 1998. *Ground water and surface water—a single resource*. U.S. Geological Survey Circular 1139.
- Winter, T.C. 2007. The role of ground water in generating streamflow in headwater areas and in maintaining baseflow. *Journal of the American Water Resources Association* 43, no.1: 15-25.

Appendices

Appendix A: Raw Data

Table 3. Raw velocity measurements, including distance from the bank and water depth at each point of measure, for Site 2 in Ramsay Prong on 10 April 2007.

Date: 10 April 2007		Time: 4:30pm			
Sample No.	Distance from Bank, b (ft)	Water Depth, h (ft)	Velocity, v (ft/s)		
			Trial 1	Trial 2	Trial 3
1	0	0.00	0.00	0.00	0.00
2	2	0.40	0.08	0.06	0.04
3	4	0.30	0.03	0.05	0.02
4	6	0.30	0.04	0.02	0.01
5	8	1.00	-0.04	-0.01	-0.04
6	10	1.10	0.10	0.10	0.07
7	12	1.10	0.10	0.11	0.09
8	14	0.60	0.32	0.23	0.20
9	16	0.00	0.00	0.00	0.00
10	18	0.70	0.27	0.27	0.28
11	20	0.00	0.00	0.00	0.00
Average (ft):		0.50			

Table 4. Raw velocity measurements, including distance from the bank and water depth at each point of measure, for Site 2 in Ramsay Prong on 10 July 2007.

Date: 10 July 2007		Time: 1:24pm			
Sample No.	Distance from Bank, b (ft)	Water Depth, h (ft)	Velocity, v (ft/s)		
			Trial 1	Trial 2	Trial 3
1	0	0.00	0.00	0.00	0.00
2	1	0.20	0.00	-0.04	-0.02
3	2	0.20	0.00	-0.02	-0.01
4	3	0.00	0.00	0.00	0.00
5	4	0.00	0.00	0.00	0.00
6	5	0.20	0.91	0.86	0.90
7	6	0.00	0.00	0.00	0.00
8	7	0.00	0.00	0.00	0.00
9	8	0.00	0.00	0.00	0.00
10	9	0.00	0.00	0.00	0.00
11	10	0.00	0.00	0.00	0.00
12	11	0.00	0.00	0.00	0.00
13	12	0.50	0.89	0.90	0.91
14	13	0.40	0.76	0.75	0.74
15	14	0.70	0.21	0.34	0.24
16	15	0.60	0.41	0.33	0.38
17	16	0.70	0.56	0.73	0.68
18	17	0.80	0.74	0.75	0.73
19	18	0.45	0.71	0.67	0.65
20	19	0.55	0.45	0.46	0.44
21	20	0.70	0.45	0.49	0.47
22	21	0.10	0.29	0.33	0.37
23	22	0.80	0.21	0.25	0.45
24	23	1.00	0.25	0.27	0.18
25	24	0.00	0.00	0.00	0.00
Average (ft):		0.32			

Table 5. Raw velocity measurements, including distance from the bank and water depth at each point of measure, for Site 2 in Ramsay Prong on 7 August 2007.

Date: 7 August 2007		Time: 2:00pm			
Sample No.	Distance from Bank, b (ft)	Water Depth, h (ft)	Velocity, v (ft/s)		
			Trial 1	Trial 2	Trial 3
1	0	0.00	0.00	0.00	0.00
2	1	0.00	0.00	0.00	0.00
3	2	0.00	0.00	0.00	0.00
4	3	0.00	0.00	0.00	0.00
5	4	0.10	-0.08	-0.07	-0.07
6	5	0.00	0.00	0.00	0.00
7	6	0.00	0.00	0.00	0.00
8	7	0.00	0.00	0.00	0.00
9	8	0.00	0.00	0.00	0.00
10	9	0.00	0.00	0.00	0.00
11	10	0.00	0.00	0.00	0.00
12	11	0.00	0.00	0.00	0.00
13	12	0.00	0.00	0.00	0.00
14	13	0.90	0.36	0.41	0.42
15	14	0.25	0.74	0.75	0.73
16	15	0.00	0.00	0.00	0.00
17	16	0.00	0.00	0.00	0.00
18	16.5	0.25	0.61	0.60	0.60
19	17	0.70	0.39	0.38	0.40
20	18	0.80	0.22	0.22	0.23
21	19	0.60	0.08	0.07	0.06
22	20	0.90	0.01	0.01	-0.01
23	21	0.70	0.11	0.12	0.12
24	22	0.80	0.15	0.17	0.18
25	23	1.00	0.21	0.22	0.22
26	24	0.70	0.11	0.12	0.10
27	25	0.00	0.00	0.00	0.00
Average (ft):		0.29			

Table 6. Raw velocity measurements, including distance from the bank and water depth at each point of measure, for Site 3 in Ramsay Prong on 10 April 2007.

Date: 10 April 2007		Time: 2:35pm			
Sample No.	Distance from Bank, b (ft)	Water Depth, h (ft)	Velocity, v (ft/s)		
			Trial 1	Trial 2	Trial 3
1	0	0.00	0.00	0.00	0.00
2	1	0.35	0.06	0.05	0.02
3	2	0.00	0.00	0.00	0.00
4	3	0.50	0.29	0.32	0.38
5	4	0.55	0.05	0.07	0.09
6	5	0.50	0.20	0.18	0.19
7	6	0.00	0.00	0.00	0.00
8	7	0.60	0.35	0.38	0.51
9	8	2.05	1.95	0.81	0.75
10	9	1.00	0.32	0.27	0.26
11	10	0.20	1.33	1.37	1.47
12	11	0.20	0.77	0.79	0.82
13	12	0.35	-0.10	-0.09	-0.07
14	13	0.00	0.00	0.00	0.00
15	14	0.00	0.00	0.00	0.00
16	15	0.00	0.00	0.00	0.00
17	16	0.00	0.00	0.00	0.00
18	17	0.00	0.00	0.00	0.00
19	18	0.40	-0.14	-0.12	-0.13
20	19	0.20	-0.02	-0.04	-0.07
21	20	0.00	0.00	0.00	0.00
Average (ft):		0.33			

Table 7. Raw velocity measurements, including distance from the bank and water depth at each point of measure, for Site 3 in Ramsay Prong on 10 July 2007.

Date: 10 July 2007		Time: 11:30am			
Sample No.	Distance from Bank, b (ft)	Water Depth, h (ft)	Velocity, v (ft/s)		
			Trial 1	Trial 2	Trial 3
1	0	0.00	0.00	0.00	0.00
2	1	0.00	0.00	0.00	0.00
3	2	0.60	-0.16	-0.16	-0.16
4	3	0.70	0.66	0.72	0.75
5	4	0.75	0.16	0.23	0.30
6	5	0.20	0.72	0.59	0.52
7	6	0.80	0.56	0.52	0.52
8	7	0.30	0.43	0.46	0.43
9	8	1.00	0.59	0.69	0.66
10	9	1.20	0.75	0.79	0.75
11	10	0.60	1.12	0.98	0.95
12	11	0.40	0.98	0.95	0.89
13	12	1.00	0.82	0.66	0.62
14	13	0.40	0.36	0.33	0.16
15	14	0.80	0.13	0.20	0.00
16	15	0.00	0.00	0.00	0.00
17	16	0.00	0.00	0.00	0.03
18	17	0.40	0.36	0.23	0.07
19	18	0.40	-0.10	-0.07	0.03
20	19	0.90	0.10	0.07	0.10
21	20	0.30	0.10	0.13	0.00
22	21	0.00	0.00	0.00	0.00
Average (ft):		0.49			

Table 8. Raw velocity measurements, including distance from the bank and water depth at each point of measure, for Site 3 in Ramsay Prong on 7 August 2007.

Date: 7 August 2007		Time: 2:35pm			
Sample No.	Distance from Bank, b (ft)	Water Depth, h (ft)	Velocity, v (ft/s)		
			Trial 1	Trial 2	Trial 3
1	0	0.00	0.00	0.00	0.00
2	1	0.70	0.06	0.06	0.07
3	2	0.60	0.05	0.05	0.04
4	3	0.40	-0.28	-0.27	-0.26
5	4	0.65	0.07	0.06	0.05
6	5	0.80	0.33	0.37	0.40
7	6	1.05	0.68	0.70	0.79
8	7	1.20	0.24	0.36	0.38
9	8	0.30	0.95	1.10	0.88
10	9	0.00	0.00	0.00	0.00
11	10	0.00	0.00	0.00	0.00
Average (ft):		0.52			

Table 9. Raw velocity measurements, including distance from the bank and water depth at each point of measure, for Site 4 in Ramsay Prong on 10 April 2007.

Date: 10 April 2007		Time: 1:55pm			
Sample No.	Distance from Bank, b (ft)	Water Depth, h (ft)	Velocity, v (ft/s)		
			Trial 1	Trial 2	Trial 3
1	0	0.00	0.00	0.00	0.00
2	1	0.95	-0.13	-0.14	-0.13
3	2	1.30	0.11	0.14	0.07
4	3	1.20	0.34	0.30	0.36
5	4	2.60	1.43	1.42	1.33
6	5	0.00	0.00	0.00	0.00
7	6	0.00	0.00	0.00	0.00
8	7	0.00	0.00	0.00	0.00
9	8	1.25	0.21	0.15	0.23
10	9	1.80	0.27	0.26	0.28
11	10	1.25	0.20	0.18	0.20
12	11	1.35	0.19	0.13	0.16
13	12	0.95	0.02	0.01	0.02
14	13	0.75	0.03	0.04	0.05
15	14	0.00	0.00	0.00	0.00
16	15	0.60	0.37	0.36	0.34
17	16	0.00	0.00	0.00	0.00
18	17	0.00	0.00	0.00	0.00
Average (ft):		0.78			

Table 10. Raw velocity measurements, including distance from the bank and water depth at each point of measure, for Site 4 in Ramsay Prong on 10 July 2007.

Date: 10 July 2007		Time: 10:55am			
Sample No.	Distance from Bank, b (ft)	Water Depth, h (ft)	Velocity, v (ft/s)		
			Trial 1	Trial 2	Trial 3
1	0	0.00	0.00	0.00	0.00
2	1	0.00	0.00	0.00	0.00
3	2	0.00	0.00	0.00	0.00
4	3	0.00	0.00	0.00	0.00
5	4	0.00	0.00	0.00	0.00
6	5	0.00	0.00	0.00	0.00
7	6	0.00	0.00	0.00	0.00
8	7	0.75	2.89	2.79	2.99
9	8	1.00	2.36	1.94	2.13
10	9	0.20	1.38	1.31	1.41
11	10	0.05	1.61	1.21	1.28
12	11	0.00	0.00	0.00	0.00
13	12	0.00	0.00	0.00	0.00
14	13	0.00	0.00	0.00	0.00
15	14.5	1.00	2.82	2.72	2.99
16	15	0.00	0.00	0.00	0.00
Average (ft):		0.19			

Table 11. Raw velocity measurements, including distance from the bank and water depth at each point of measure, for Site 4 in Ramsay Prong on 7 August 2007.

Date: 7 August 2007		Time: 11:45am			
Sample No.	Distance from Bank, b (ft)	Water Depth, h (ft)	Velocity, v (ft/s)		
			Trial 1	Trial 2	Trial 3
1	0	0.00	0.00	0.00	0.00
2	1	0.95	-0.08	-0.07	-0.09
3	2	1.10	0.07	0.04	0.05
4	3	0.60	2.57	2.59	2.67
5	4	1.00	-0.25	-0.26	-0.30
6	5	0.10	0.10	0.17	0.11
7	6	0.20	1.42	1.44	1.38
8	7	0.20	0.72	0.75	0.78
9	8	0.25	-0.13	-0.11	-0.12
10	9	0.40	0.67	0.88	1.05
11	10.5	0.10	0.41	0.44	0.45
12	11	0.00	0.00	0.00	0.00
Average (ft):		0.41			

Table 12. Raw velocity measurements, including distance from the bank and water depth at each point of measure, for Site 5 in Ramsay Prong on 10 April 2007.

Date: 10 April 2007		Time: 12:21pm			
Sample No.	Distance from Bank, b (ft)	Water Depth, h (ft)	Velocity, v (ft/s)		
			Trial 1	Trial 2	Trial 3
1	0	0.00	0.00	0.00	0.00
2	2	0.90	0.59	0.56	0.57
3	4	0.70	0.33	0.34	0.37
4	6	0.00	0.00	0.00	0.00
5	8	0.00	0.00	0.00	0.00
6	10	0.20	0.20	0.20	0.20
7	12	0.80	-0.15	-0.18	-0.20
8	14	1.00	0.41	0.42	0.37
9	16	1.50	-0.13	-0.09	-0.11
10	18	1.50	0.40	0.33	0.31
11	20	1.80	0.07	0.04	0.03
12	22	0.60	-0.42	-0.39	-0.37
13	24	0.20	0.03	0.02	0.01
14	26	0.00	0.00	0.00	0.00
Average (ft):		0.66			

Table 13. Raw velocity measurements, including distance from the bank and water depth at each point of measure, for Site 5 in Ramsay Prong on 7 August 2007.

Date: 7 August 2007		Time: 10:17am			
Sample No.	Distance from Bank, b (ft)	Water Depth, h (ft)	Velocity, v (ft/s)		
			Trial 1	Trial 2	Trial 3
1	0	0.00	0.00	0.00	0.00
2	1	1.20	0.56	0.50	0.43
3	3	0.50	0.31	0.27	0.25
4	5	0.70	0.76	0.74	0.72
5	7.5	1.50	0.53	0.54	0.54
6	9	0.00	0.00	0.00	0.00
7	11	0.70	-0.09	-0.10	-0.10
8	13	1.20	-0.17	-0.14	-0.13
9	15	1.80	-0.22	-0.17	-0.16
10	17	1.30	0.05	0.03	0.06
11	19	1.50	0.10	0.05	0.04
12	21	1.80	-0.23	-0.23	-0.24
13	23	0.50	-0.17	-0.18	-0.18
14	25	0.20	-0.18	-0.16	-0.15
15	27	0.00	0.00	0.00	0.00
Average (ft):		0.86			

Table 14. Raw velocity measurements, including distance from the bank and water depth at each point of measure, for Site 6 in Ramsay Prong on 10 April 2007.

Date: 10 April 2007		Time: 11:35am			
Sample No.	Distance from Bank, b (ft)	Water Depth, h (ft)	Velocity, v (ft/s)		
			Trial 1	Trial 2	Trial 3
1	0	0.00	0.00	0.00	0.00
2	4	0.00	0.00	0.00	0.00
3	5	1.00	-0.13	-0.18	-0.16
4	6	0.90	-0.09	-0.12	-0.15
5	7	1.10	2.49	2.57	1.94
6	8	1.15	1.76	1.81	1.93
7	9	0.00	0.00	0.00	0.00
8	10	0.30	-0.26	-0.27	-0.22
9	11	0.25	-0.11	-0.03	-0.04
10	12	0.50	0.29	0.31	0.25
11	13	0.60	0.79	0.56	0.60
12	14	0.55	-0.16	-0.13	-0.14
13	15	0.00	0.00	0.00	0.00
Average (ft):		0.49			

Table 15. Raw velocity measurements, including distance from the bank and water depth at each point of measure, for Site 6 in Ramsay Prong on 7 August 2007.

Date: 7 August 2007		Time: 9:48am			
Sample No.	Distance from Bank, b (ft)	Water Depth, h (ft)	Velocity, v (ft/s)		
			Trial 1	Trial 2	Trial 3
1	0	0.00	0.00	0.00	0.00
2	1	0.00	0.00	0.00	0.00
3	2	0.10	0.28	0.33	0.46
4	3	0.40	2.08	3.59	1.74
5	4	0.30	3.32	3.04	1.73
6	5	0.00	0.00	0.00	0.00
7	6	1.30	0.65	1.16	0.57
8	7	0.55	1.94	1.31	1.98
9	8	0.40	0.55	0.48	1.10
10	9	1.00	1.18	0.61	0.65
11	10	0.50	2.92	3.08	2.93
12	11	1.00	1.01	1.64	1.34
13	12	0.30	-0.36	-0.08	-0.10
14	13	0.00	0.00	0.00	0.00
15	14	0.00	0.00	0.00	0.00
16	15	0.60	1.77	1.18	1.10
17	16	0.00	0.00	0.00	0.00
Average (ft):		0.38			

Table 16. Raw velocity measurements, including distance from the bank and water depth at each point of measure, for Site 7 in Ramsay Prong on 10 April 2007.

Date: 10 April 2007		Time: 9:45am			
Sample No.	Distance from Bank, b (ft)	Water Depth, h (ft)	Velocity, v (ft/s)		
			Trial 1	Trial 2	Trial 3
1	0	0.00	0.00	0.00	0.00
2	8	0.00	0.00	0.00	0.00
3	13	1.45	0.87	0.86	1.09
4	15	0.35	1.20	1.58	1.43
5	17	0.12	0.08	0.12	0.13
6	19	0.19	-0.37	-0.03	-0.35
7	21	0.00	0.00	0.00	0.00
8	23	0.45	1.59	1.92	1.67
9	25	0.00	0.00	0.00	0.00
10	27	0.60	0.43	0.56	0.48
11	29	0.20	1.13	0.97	1.20
12	31	0.23	0.14	0.18	0.27
13	33	0.10	0.00	0.00	0.00
14	35	0.00	0.00	0.00	0.00
15	37	0.00	0.00	0.00	0.00
16	39	0.00	0.00	0.00	0.00
17	41	0.60	-0.05	-0.04	-0.02
18	43	0.00	0.00	0.00	0.00
Average (ft):		0.24			

Table 17. Raw velocity measurements, including distance from the bank and water depth at each point of measure, for Site 7 in Ramsay Prong on 10 July 2007.

Date: 10 July 2007		Time: 8:58am			
Sample No.	Distance from Bank, b (ft)	Water Depth, h (ft)	Velocity, v (ft/s)		
			Trial 1	Trial 2	Trial 3
1	0	0.00	0.00	0.00	0.00
2	2	0.25	0.13	0.16	0.13
3	4	0.00	0.00	0.00	0.00
4	6	0.00	0.00	0.00	0.00
5	8	0.30	-0.33	-0.26	-0.26
6	10	0.50	1.08	1.12	1.12
7	12	0.90	1.64	1.61	1.64
8	14	0.60	-0.56	-0.49	-0.36
9	16	0.00	0.00	0.00	0.00
10	18	0.00	0.00	0.00	0.00
11	20	0.00	0.00	0.00	0.00
12	22	0.00	0.00	0.00	0.00
13	24	0.00	0.00	0.00	0.00
14	26	0.10	0.62	0.49	0.56
15	28	0.00	0.00	0.00	0.00
16	30	0.00	0.00	0.00	0.00
17	32	0.60	-0.16	-0.20	-0.13
18	34	0.60	0.36	0.33	0.39
19	36	0.40	1.12	1.02	1.02
20	38	0.50	0.33	0.36	0.56
21	40	0.00	0.00	0.00	0.00
22	42	0.00	0.00	0.00	0.00
Average (ft):		0.22			

Table 18. Raw velocity measurements, including distance from the bank and water depth at each point of measure, for Site 7 in Ramsay Prong on 7 August 2007.

Date: 7 August 2007		Time: 8:30am			
Sample No.	Distance from Bank, b (ft)	Water Depth, h (ft)	Velocity, v (ft/s)		
			Trial 1	Trial 2	Trial 3
1	0	0.00	0.00	0.00	0.00
2	1	0.10	-0.02	-0.02	-0.02
3	3	0.60	-0.03	-0.07	0.02
4	5	0.70	0.01	-0.04	-0.06
5	7	0.90	-0.22	-0.16	-0.17
6	9	2.05	0.32	0.28	0.28
7	11	1.85	0.41	0.45	0.91
8	13	1.10	0.91	0.96	0.90
9	15	2.00	0.86	0.96	0.99
10	17	1.90	0.49	0.44	0.85
11	19	1.10	0.38	0.65	0.12
12	21	0.00	0.00	0.00	0.00
13	23	0.00	0.00	0.00	0.00
14	25	2.30	2.77	2.32	2.93
15	27	0.00	0.00	0.00	0.00
16	29	0.00	0.00	0.00	0.00
17	31	0.70	0.18	0.20	0.21
18	33	0.00	0.00	0.00	0.00
19	35	0.20	0.61	0.66	0.73
20	37	0.55	0.55	0.70	1.06
21	39	0.00	0.00	0.00	0.00
Average (ft):		0.76			

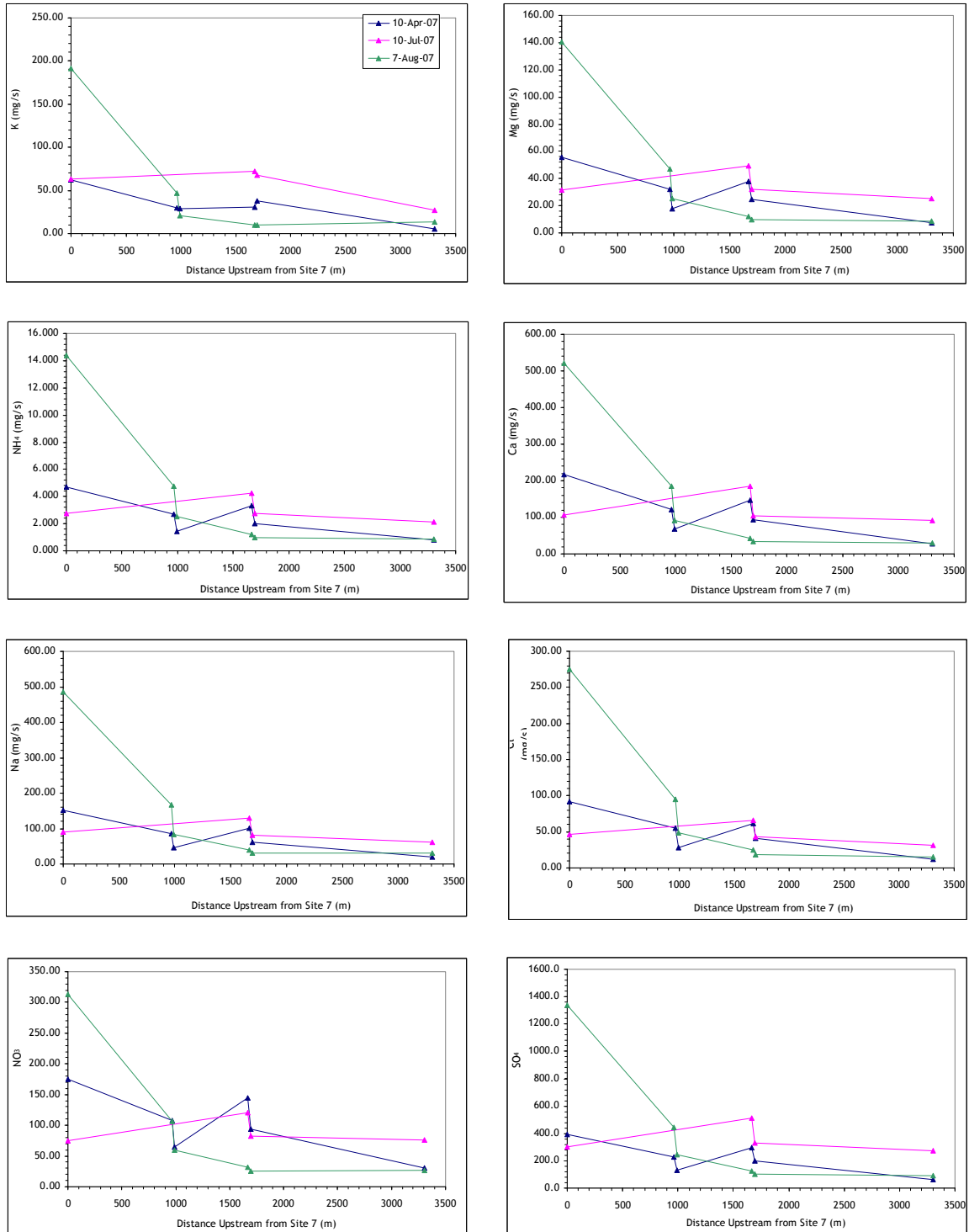


Figure 14. Mass loading rates with distance upstream from Site 7 for major ions in Ramsay Prong, tributaries, and adjacent springs on each monitoring day.

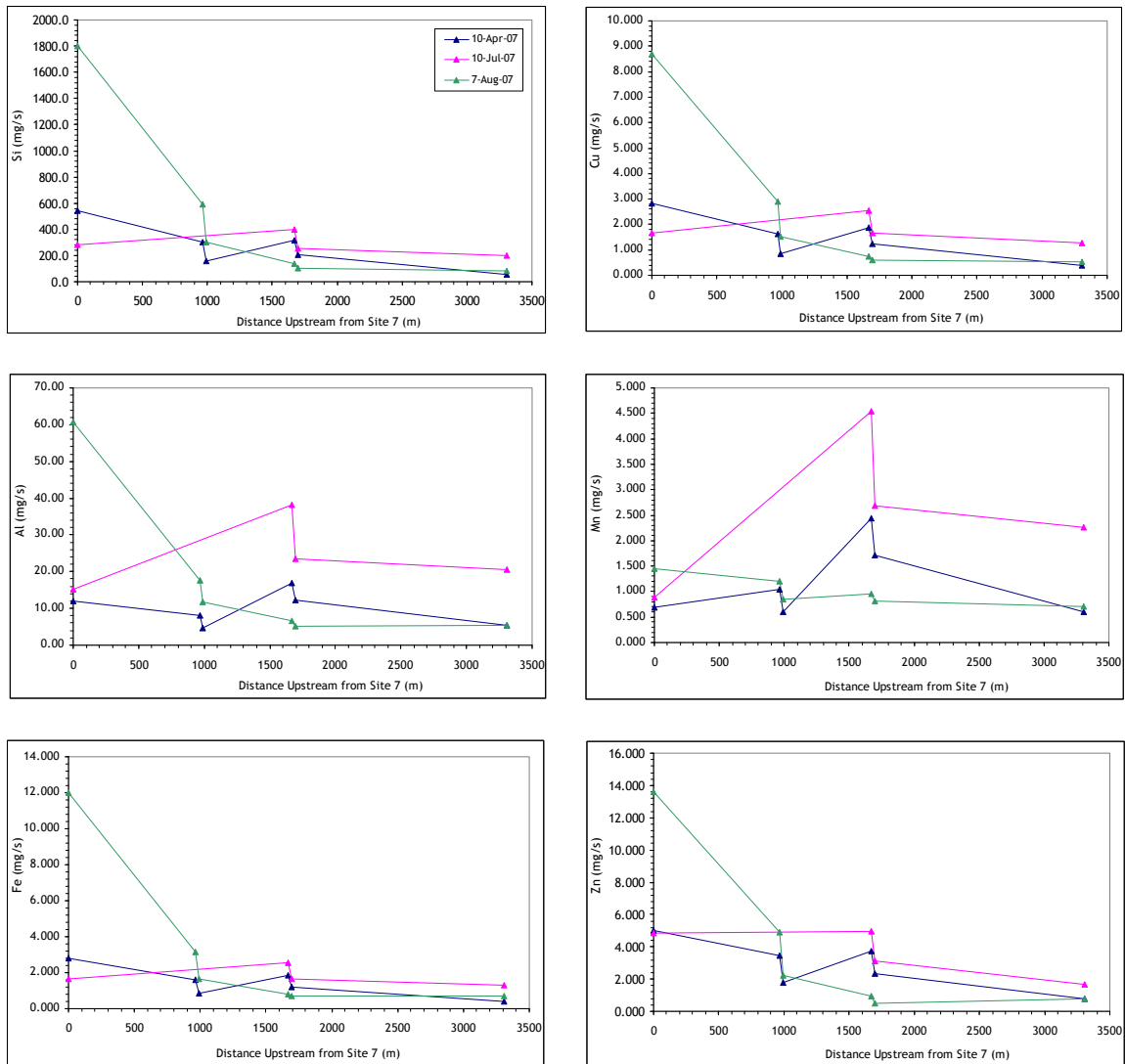


Figure 15. Mass loading rates with distance upstream from Site 7 for trace metals and total silica in Ramsay Prong, tributaries, and adjacent springs on each monitoring day.

Table 19. Water quality parameters recorded in precipitation throughfall near Site 6 on the bank of Ramsay Prong.

Date	Conductivity μS/cm	pH	ANC μeq/L
06/01/06	19.11	4.73	152.18
06/28/06	16.46	6.24	55.26
07/31/06	19.67	5.83	27.48
09/08/06	17.96	6.01	37.75
09/30/06	14.63	6.17	47.22
11/03/06	24.60	5.54	37.98
12/01/06	12.36	5.47	18.29
01/02/07	13.94	5.14	4.66
02/09/07	13.41	5.45	9.96
02/28/07	30.20	5.18	8.44
03/03/07	13.29	5.08	6.85
03/16/07	19.69	4.93	-0.55
04/29/07	47.70	6.01	157.44
05/30/07	33.40	6.66	162.39
06/15/07	25.50	6.09	56.98
06/21/07	17.86	6.05	38.80
07/03/07	12.98	5.02	-4.54

Table 20. Concentrations of major ions recorded in precipitation throughfall near Site 6 on the bank of Ramsay Prong.

Date	Cl μeq/L	NO ₃ -N μeq/L	SO ₄ μeq/L	NH ₄ -N μeq/L	H μeq/L	Na μeq/L	K μeq/L	Mg μeq/L	Ca μeq/L
06/01/06	24.65	13.94	35.79	24.48	18.45	28.48	65.24	15.96	30.92
06/28/06	6.80	3.32	36.61	3.04	0.58	5.66	68.69	22.86	25.40
07/31/06	8.48	10.95	69.64	18.40	1.46	6.23	46.57	21.54	34.52
09/08/06	3.87	5.36	64.90	1.14	0.98	3.74	62.35	20.96	51.60
09/30/06	7.26	4.50	39.92	8.19	0.68	2.73	63.66	13.35	35.50
11/03/06	12.27	1.13	48.57	0.06	2.90	5.56	147.00	36.08	26.99
12/01/06	9.45	5.10	35.31	4.70	3.42	6.10	35.76	14.87	28.83
01/02/07	10.74	12.16	42.48	1.23	7.27	5.91	35.41	14.46	43.32
02/09/07	19.20	7.00	40.31	0.98	3.54	10.75	31.81	16.11	46.44
02/28/07	71.50	30.66	81.18	18.55	6.64	65.63	53.35	32.27	91.72
03/03/07	12.04	7.80	30.44	6.00	8.25	11.67	27.80	14.57	51.40
03/16/07	21.29	4.29	53.09	5.44	11.66	16.27	53.96	23.41	56.94
04/29/07	41.03	45.11	109.41	14.45	0.97	29.92	62.98	75.54	192.78
05/30/07	13.46	4.50	74.93	14.45	0.22	13.27	89.65	66.12	115.47
06/15/07	11.93	24.53	79.20	NR	0.81	8.99	87.29	35.99	60.97
06/21/07	12.54	2.54	55.69	1.02	0.88	12.04	63.14	23.94	57.40
07/03/07	17.24	14.81	41.67	9.37	NR	NR	NR	NR	NR

Table 21. Trace metals recorded in precipitation throughfall near Site 6 on the bank of Ramsay Prong.

Date	Al	Cu	Fe	Mn	Si	Zn
	ppm	ppm	ppm	ppm	ppm	ppm
06/01/06	0.14	BDL	0.11	0.03	0.36	0.02
06/28/06	0.03	BDL	0.02	0.02	0.06	0.04
07/31/06	0.23	BDL	0.03	0.04	0.02	0.08
09/08/06	0.03	BDL	BDL	0.03	0.15	0.42
09/30/06	0.03	BDL	BDL	0.02	0.11	0.35
11/03/06	0.06	BDL	0.02	0.13	0.04	BDL
12/01/06	BDL	0.04	BDL	0.04	BDL	0.06
01/02/07	BDL	BDL	BDL	0.04	0.02	0.07
02/09/07	BDL	BDL	BDL	0.03	BDL	0.11
02/28/07	0.02	BDL	0.01	0.03	BDL	0.22
03/03/07	0.03	BDL	BDL	0.03	0.03	0.12
03/16/07	0.08	BDL	0.01	0.06	BDL	0.06
04/29/07	0.03	BDL	0.03	0.09	0.06	0.33
05/30/07	0.04	BDL	0.23	BDL	0.06	0.17
06/15/07	BDL	BDL	BDL	0.01	0.16	0.24
06/21/07	0.02	BDL	BDL	0.01	0.09	0.27
07/03/07	NR	NR	NR	NR	NR	NR

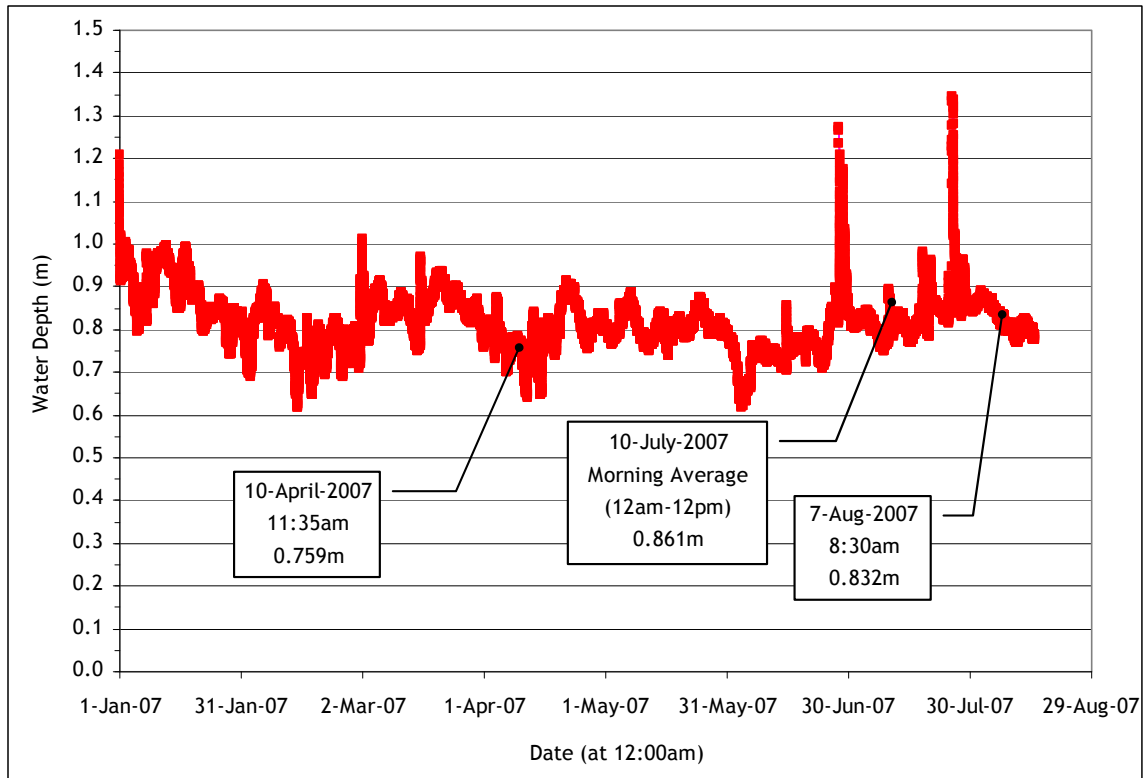


Figure 16. Ramsay Prong stage data measured at 15-minute intervals by the UT monitoring station sonde situated approximately 0.1mi downstream from Site 6.

Appendix B: Sample Calculations

B.1 Ramsay Prong Discharge

For a rectangular (inner) section:

$$Q_x = 0.5(b_{x+1} - b_{x-1})V_x h_x$$

where Q_x = discharge through the partial section x, L/s
 b_{x+1} = distance from bank to next point of measure x+1, m
 b_{x-1} = distance from bank to preceding point of measure x-1, m
 h_x = depth of water throughout the partial section x, m
 V_x = average velocity through the partial section x, m/s

For a trapezoidal (end) section:

$$Q_1 = 0.5(b_2 - b_1)V_1 h_1$$

$$Q_n = 0.5(b_n - b_{n-1})V_n h_n$$

Total Discharge:

$$Q_T = \sum_{x=1}^n Q_x$$

where Q_T = discharge through the partial section x, L/s

B.2 Mass Loading Rate

For major ions:

$$q_i = QC_i M_w M_c$$

where q_i = mass loading rate of ion i, mg/s
 Q = flow rate at point of measure, L/s
 C_i = concentration of ion i recorded at point of measure, eq/L
 M_w = molecular weight of ion, g/mol
 M_c = molecular charge of ion, eq/mol

For metals:

$$q_i = QC_iM_w$$

where q_i = mass loading rate of specie i, mg/s
 Q = flow rate at point of measure, L/s
 C_i = concentration of ion i recorded at point of measure, mg/L

Vita

Amanda Marie McKenna was born in Parma, OH on 7 October 1982. Raised in North Olmsted, Ohio, Amanda was educated in the city's public school system, graduating with honors from North Olmsted High School in 2001. She then spent a year at the University of Findlay (Findlay, OH) and in August 2002 transferred to Michigan Technological University (Houghton, MI) where she graduated *magna cum laude* with a B.S. in Environmental Engineering in 2005. During her undergraduate career, Amanda held three internships: as a water resources undergraduate researcher at Clarkson University (Potsdam, NY) for the National Science Foundation's Research Experience for Undergraduates (REU) Program, as a co-op student in the Environmental, Safety & Health Department at Cargill, Inc.'s North America Sweeteners facility (Eddyville, IA), and as a water quality intern for the Minnesota Department of Health (International Falls, MN). In 2007, Amanda earned an M.S. in Environmental Engineering with a focus in Water Resources from the University of Tennessee (Knoxville, TN). She currently holds the position of Research Associate at the Center for Clean Products at the Institute for a Secure and Sustainable Environment, a research organization at The University of Tennessee—Knoxville.